OXYGEN SOLUBILITY IN LIQUID IRON AND IRON-CHROMIUM ALLOYS

THE SOLUBILITY OF OXYGEN IN LIQUID IRON
AND
IRON-CHROMIUM ALLOYS

By

FRANCIS CLEMENT LOUIS LARCHÉ,
Ingenieur Civil des Mines

A Thesis
Submitted to the Faculty of Graduate Studies
in Partial Fulfilment of the Requirements
for the Degree
Master of Science

McMaster University
August 1968

MASTER OF SCIENCE (1968)
(Metallurgy)

McMASTER UNIVERSITY
Hamilton, Ontario.

TITLE: The Solubility of Oxygen in Liquid Iron and Liquid Iron-Chromium Alloys

AUTHOR: Francis Clement Louis Larché, Ingenieur Civil des Mines

SUPERVISOR: Dr. A. McLean

NUMBER OF PAGES: xii, 60

SCOPE AND CONTENTS:

Levitation melting was used to measure the equilibrium between H_2-H_2O or CO-CO_2 gas mixtures and pure Fe or Fe-Cr alloys over the temperature range 1550 - 1750°C. The effects of thermal diffusion on the two types of gases were investigated.

First and second order interaction parameters were employed to describe the interaction between oxygen and chromium (up to 25 wt. pct. of Cr.).

ACKNOWLEDGEMENTS

The author wishes to express his sincere gratitude to his research supervisor, Dr. A. McLean, whose assistance and encouragement led to a successful completion of the work.

In addition, the author would like to thank Mr. H. Neumayer whose technical suggestions and assistance allowed the experimental work to be performed efficiently.

Thanks are also due to Mrs. A. Miltimore for her skillful typing.

Financial assistance was obtained through the National Research Council and the Canada Council.

TABLE OF CONTENTS

TABLES

FIGURES

LIST OF TABLES

LIST OF FIGURES

Figure

LIST OF SYMBOLS

k	Boltzman's constant
m	mass
s	surface area
T	absolute temperature
v	volume
a_M	activity of component M
$e_i^{(j)}$	First order free energy interaction coefficient. wt. pct. scale.
f_G	fugacity of gas G
f_o	activity coefficient of oxygen in liquid iron-wt. pct. scale
$h_i^{(j)}$	first order enthalpy interaction coefficient. wt. pct. scale
K_1	Equilibrium constant for the reaction $H_2 + \underline{O} = H_2O$
K'_1	pseudo equilibrium constant for the reaction $H_2 + \underline{O} = H_2O$
K_2	Equilibrium constant for the reaction $CO + \underline{O} = CO_2$
K'_2	pseudo equilibrium constant for the reaction $CO + \underline{O} = CO_2$
K_3	equilibrium constant for the reaction $Cr_3O_4 = 3\ \underline{Cr} + 4\ \underline{O}$
$\ell_i^{(j)}$	second order enthalpy interaction coefficient. wt. pct. scale
M_1	atomic weight of the solvent in a mixture
M_j	Atomic weight of solute j in a mixture
$p_i^{(j)}$	Second order entropy interaction coefficient. wt. pct. scale
P_G	Pressure of gas G
$r_i^{(j)}$	Second order free energy interaction coefficient. wt. pct. scale
$r_i^{(j,k)}$	Second order free energy interaction coefficient. Cross term. wt. pct. scale.

$s_i^{(j)}$	first order entropy interaction coefficient - wt. pct. scale.
X_j	mole fraction of component j.
γ_i	activity coefficient of i; mole fraction scale.
$\delta_i^{(j)}$	first order entropy interaction coefficient - mole fraction scale.
$\varepsilon_i^{(j)}$	first order free energy interaction coefficient. Mole fraction scale.
$\eta_i^{(j)}$	first order enthalpy interaction coefficient. Mole fraction scale.
$\lambda_i^{(j)}$	second order enthalpy interaction coefficient. Mole fraction scale.
$\pi_i^{(j)}$	second order entropy interaction coefficient - mole fraction scale.
ρ	density
$\rho_i^{(j)}$	second order free energy interaction coefficient. Mole fraction scale.
$\rho_i^{(j,k)}$	second order free energy interaction coefficient. cross term - mole fraction scale.
ΔG^o	Standard free energy change for a chemical reaction
ΔH^o	Standard enthalpy change for a chemical reaction
ΔS^o	Standard entropy change for a chemical reaction

Underlined elements like $\underline{Cr}$ or $\underline{O}$ refer to the elements dissolved in liquid iron

INTRODUCTION

Levitation melting techniques have already been used several times for studying gas-metal reactions. Kinetics of dissolution and equilibrium constants have been determined with this method. In connection with this technique the use of gas mixtures may introduce phenomena, for example thermal diffusion,which can produce misleading results.

Following Richardson, who studied the system Cu-O and Ni-O with $CO-CO_2$ gas mixtures, the purpose of this investigation was

i) to study the parameters influencing the dissolution of oxygen in liquid iron from $CO-CO_2$ and H_2-H_2O gas mixtures

ii) to investigate these effects when an alloying element is present in the liquid iron.

The allowing element chosen was chromium. Data from several sources over the range 0 - 10 wt. pct. chromium were available for comparison. The present study was expected to provide data up to 25 wt. pct. chromium.

In the past, the effect of chromium on the behaviour of oxygen has been studied only at temperatures close to $1600^{\circ}C$. An objective of this work was to determine the effect of temperature on chromium-oxygen interactions over the range 1550 - $1750^{\circ}C$.

This information would provide a basis for the construction of a chromium-oxygen-chromium oxide equilibrium diagram which would be of value when considering the reactions involved in stainless steelmaking.

CHAPTER I

Literature Review

1.1 Thermodynamics of liquid metallic solutions - Introduction

The thermodynamic description of liquid metallic solutions consists essentially in obtaining a suitable analytical representation for the activities of the various components of the mixture.

This representation has to be:

- thermodynamically consistent;
- in agreement with the limiting laws for the solutes and the solvent (Henry's and Raoult's laws).

For convenience, it should be as simple as possible and compatible with the precision of the experimental data.

No representation is actually satisfactory over the whole range of concentrations. Wagner's formalism for dilute solutions and Lupis' extension will be briefly reviewed here.

1.2 Interaction formalism

Wagner(1) and Chipman(2) represent the excess free energy of component i in a dilute multi-component solution by a Taylor series expansion. They develop the formalism of the first order interaction coefficient:

$$\varepsilon_i^{(j)} = \frac{\partial \ln \gamma_i}{\partial x_j} \tag{1.1}$$

Later Lupis and Elliott(4,5) expand this treatment to higher order interaction parameters, as well as enthalpy and entropy interaction coefficients.

Although the molar fraction is the more fundamental composition unit, it is some times more convenient to use other units. The notations for these various interaction coefficients are grouped in Table I, along with the representative equations of the excess free energy of component i.

The conversion of these parameters from the weight percent coordinates to the mole fraction coordinates (Lupis and J. F. Elliott(3,4,5)) is shown below. Some useful thermodynamic relationships between these quantities are also given.

$$\varepsilon_i^{(j)} = 230 \frac{M_j}{M_1} e_i^{(j)} + \frac{M_1 - M_j}{M_1} \tag{1.2}$$

$$\rho_i^{(j)} = \frac{2.3 \times 10^2}{M_1^2} [10^2 M_j^2 r_i^{(j)} + M_j (M_1 - M_j) e_i^{(j)}] + \frac{1}{2} (\frac{M_1 - M_j}{M_1})^2 \tag{1.3}$$

$$\varepsilon_i^{(j)} = \frac{\eta_i^{(j)}}{RT} - \frac{\delta_i^{(j)}}{R} \tag{1.4}$$

$$e_i^{(j)} = \frac{h_i^{(j)}}{2.3\ RT} - \frac{s_i^{(j)}}{2.3\ R} \tag{1.5}$$

Figure (1) is a graphical representation of the first and second order free energy interaction coefficients in a ternary 1-i-j system.

1.3 The Fe-O system

Numerous investigations have been carried out on the solubility of oxygen in pure liquid iron at steelmaking temperatures. Gokcen(12), and subsequently Tankins, Gokcen and Belton(13) reviewed the literature up to 1964. J. Chipman(14) gives also references and values from the latest research work in this area. The partial pressure of oxygen in equilibrium with iron and iron oxide at 1600°C is extremely low (approximately 10^{-8} atmospheres$^{(15)}$). Because of the difficulties for controlling such a low pressure, the oxygen potential is generally fixed by a gas mixture containing H_2-H_2O or CO-CO_2, the first being the most commonly used. The reactions with the molten metal can be written as:

$$H_2 + \underline{O} = H_2O$$

$$CO + \underline{O} = CO_2$$

the underlined symbols referring to elements dissolved in liquid iron. The law of mass action can be used to write the equilibrium constants

$$K_1 = \left(\frac{f H_2O}{f H_2}\right) \frac{1}{(a_o)}$$

$$K_2 = \left(\frac{f CO_2}{f CO}\right) \frac{1}{(a_o)}$$

with the subsequent notation

$$K_1' = \frac{P_{H_2O}}{P_{H_2}} \frac{1}{(\%\ O)}$$

$$K_2' = \left(\frac{P_{CO_2}}{P_{CO}}\right) \frac{1}{(\%\ O)}$$

f_{H_2O}, f_{H_2},... are the fugacities of the gases, and a_o is the activity of oxygen in the melt. The deviation from ideality of the gases used being extremely small, fugacities and partial pressures are considered to be identical.

From the data on one gas mixture, one can, by means of thermodynamic data for the water-gas reaction

$$H_2(g) + CO_2(g) = H_2O(g) + CO(g)$$

calculate the equivalent value for the reaction with the other gas mixtures.

The values of log K_T from various investigators (converted, if necessary, from values of log K_2) are shown in Fig. 2. It is rather difficult, in view of the difficulties of experimentation at high temperature, to point out specifically the causes of the discrepancies. However, they can be attributed to four main sources:

(1) Oxygen analyses.
(2) Thermal diffusion.
(3) Temperature measurement.
(4) Crucible contamination.

(1) Oxygen analyses have been made in all investigations listed in the references (10 to 13, 16 to 23) by vacuum fusion. Gokcen(12) pointed out the possibilities of low and erratic values for samples containing over 0.02 pct O., due to spatter upon melting, when they are dropped in a graphite crucible not equipped with a baffle or a lid.

(2) When a mixture of gases encounters a hot surface with a thermal gradient, the heavier molecules tend to concentrate away from the surface. This phenomenon is called thermal diffusion, and was adequately described, in connection with gas-metal reactions by Emmet and Schultz(24), Darken and Gurry(25), Dastur and Chipman(26), Sakao and Sano(27) and by Bockris, McKenzie and White(28).

The thermal gradient above the melt is particularly high in induction heating furnaces. If thermal diffusion occurs, the ratio P_{H_2O}/P_{H_2} prevailing at the surface will be lower than the inlet ratio, thus giving high values of K_1'.

(3) Errors in optical temperature measurements can arise from large extrapolations of the calibration data. When measurements are taken by sighting directly onto the melt, emissivity and reflectivity corrections have to be made. Unexpected errors can arise in such measurements (d'Entremont(29)). Furthermore, the variation of emissivity with oxygen content is not known. Since oxygen is tensioactif(30), this change may be important.

(4) Crucible contamination can easily arise at low P_{H_2O}/P_{H_2} ratios (dissolution of oxygen from the refractory crucible) or high P_{H_2O}/P_{H_2} (formation of spinels). When induction heating is used, the melt is continuously stirred thus washing the walls of the crucible and enhancing the kinetics of the reaction.

1.4 Effect of chromium on the activity of oxygen dissolved in liquid iron

The literature on Fe-Cr-O alloys has been reviewed by Shiraishi(31) up to 1965. All the experimentations have been made with crucible techniques. They were therefore subject to the same possibilities of error as the experiments for the Fe-O system. To them, one may add the possibility of entraping oxides when suction samples are taken through a layer of slag.

Since 1966 Pargeter(32) made a somewhat limited investigation of chromium-oxygen interactions at 1600°C. The apparatus used was similar to that used by Chipman et al(21). His results are included with the results of other investigators in Table II, summarized in the form of interaction parameters.

Shiraishi(31) was the first to use a levitation melting technique for studying this system. However, it is felt that his data are insufficient to allow a good interpretation for the effect of chromium on the behaviour of oxygen dissolved in liquid iron.

CHAPTER II

Experimental Considerations

2.1 Thermal diffusion

2.1a Introduction

When a mixture of gases of different molecular weight enter a region with a thermal gradient, segregation of the mixture occurs. The heavier molecules tend to accumulate in the cooler zone. This phenomenon is called thermal diffusion. It is probably one of the most significant sources of error in the studies of gas-metal reactions at high temperatures.

Predicted by Enskog(33) in 1911 and by Chapman(34,35) in 1916, it was first observed by Chapman and Dootson(36) in 1917. The errors which can arise in static atmospheres of H_2-H_2O in studies of gas-metal equilibria can be as high as 40%. (Emmet and Schulz(24)).

Several methods have since been investigated in order to minimize its effects.

i) Darken and Gurry(37) calculate its extent in CO-CO_2 mixtures flowing through a vertical furnace.

ii) Dastur and Chipman(26) proposed two methods for a gas mixture flowing down onto the surface of an induction heated melt.

  a) Preheating the gases in order to eliminate, as far as possible, the thermal gradient near the surface.

  b) Mixing with a gas of high molecular weight. This method is based on Gillepsie's theory(18), which shows that the error in log K' should be proportional to the mean square root of the molecular weight of the mixture.

iii) Sakao and Sano(27) investigated the effect of argon additions, temperature of preheat, distance of preheater to the melt and rate of gas flow. They conclude that the effect of thermal diffusion is not as severe as Dastur and Chipman stated.

iv) Richardson and Alcock(28) discussed the effect of flow rate; they note that if an increase of four-fold in flow rate does not affect the equilibrium value, it can be assumed that thermal diffusion has no effect on the gas mixture.

2.1b Levitation melting and thermal diffusion

Richardson and Toop(39) discussed thermal diffusion in connection with levitation. They found that the steady state obtained with $CO-CO_2$ and molten nickel droplets was the same as the full equilibrium state in so far as the partition of oxygen was concerned.

Shiraishi(31) concluded that the effect was also negligible with H_2O-H_2 mixtures and molten iron droplets. However his conclusions were based on only a few experiments with levitation melting and his results could easily be misleading.

In agreement with some recent work by Kershaw(40) this study has shown that for molten iron droplets

i) thermal diffusion is negligible with $CO-CO_2$ gas mixtures

ii) its effects are important with H_2-H_2O gas mixtures

No attempt was made to minimize the effects of this phenomenon, but the pseudo-equilibrium constant can be of value in determining the effect of an alloying addition on oxygen dissolution in molten iron (cf. Chapter V).

2.2 Temperature control

One of the major problems which faced earlier investigators of levitation melting was the control of temperature of the molten metal droplet. The heat is produced in the droplet by I^2R losses of the current induced in it. The characteristics of the field and the position of the droplet in the field are therefore of prime importance for temperature control. The factors which affect them are, for a given power supply:

(1) coil current
(2) coil geometry
(3) weight of sample
(4) electrical properties of the specimen

Additional important factors are to be found in the gaseous medium surrounding the droplet (composition and flow rate).

By suitably combining these factors, levitation melting can be used over an extended range of temperatures.

In this study the power was supplied by a high frequency generator, 450 kc/s and 10 kW. A step down transformer (7.5:1) was placed between the generator and the coil, thus providing a higher current intensity in the coil. It has the further advantage of suppressing any discharges in the reaction tube.

Several coil designs were used in order to keep the flow of H_2-H_2O constant, and obtain the temperatures desired. Coils No. 1 to 3 (Fig. 3) are numbered in order of increased working temperature range. It was observed, in agreement with Richardson(39), that the temperature of the droplet passes through a minimum when, at constant power input, the distance between the levitating and stabilizing part of the coil is increased. This corresponds also to maximum mechanical stability.

The sample weight was kept between 0.5 and 1.5g. With a particular coil geometry and power input, the temperature was higher with the heavier samples. This conclusion is valid in the weight range considered in this investigation, but may not be valid on a more extended range.

Gases like hydrogen or helium, with high thermal conductivity can conveniently be used for obtaining low temperatures, with a reasonable flow rate (0.5 to 2 liters per minute). CO, CO_2, Ar and N_2 have a small effect on temperature. In order to obtain low temperatures the gas should move upward through the reaction chamber at a high flow rate (up to 20 l. per minute or more). This can give rise to mechanical instabilities, due to the large turbulence around the droplet.

2.3 Temperature measurement

In this investigation a Milletron two colour pyrometer was used. This equipment measures the ratio of energies radiated around two wavelengths (0.53 and 0.62 microns). This instrument like any other optical pyrometer has to be calibrated for any particular system. The calibration was carried out with an Fe-C alloy, held in an alumina crucible, and heated by induction (Fig. 4). The true temperature was obtained with a Platinum-6% Rh, Pt-30% Rh thermocouple. Above 1700°C, the evaporation of iron interferes with the pyrometer measurements. Therefore, calibration has to be extrapolated to 1800°C. When the temperature of the actual levitated specimen was measured, a close-up lens was used. This allowed the drop to cover the entire field of the pyrometer. Temperatures were measured from the bottom of the reaction chamber, with gas flowing upwards; in this way errors due to fume formation were eliminated.

The calibration curve was frequently checked against the melting point of 'Ferrovac E' iron (composition is shown in Table III) which was taken as 1539°C.

2.4 Oxygen and carbon analyses

The oxygen analyses were done on a LECO oxygen analyser. The principle is gaseous reducing fusion. The sample, of about one gram., is dropped into a graphite crucible, heated by induction (temperatures reached can be as high as 2600°C). The carbon monoxide is swept by a current of purified helium into a catalyst furnace. The rare earth and copper oxides oxidize CO to CO_2, which is trapped. After a preset elution time, the trap is heated, and CO_2 is passed through chromatographic columns, with helium as carrier gas. The carbon dioxide peak is integrated, and the result, converted to Wt.pct. oxygen appears directly on a digital readout.

The reproducibility of the apparatus, in the best working conditions, is about 2 p.p.m. However, the absolute value depends on the reliability of the standards (furnished by LECO). It is assumed that the error is of the order of ± 5 p.p.m. Preparation of the furnace and calibration was done by following the instructions of the manufacturer. Samples were washed in acetone, dried, and weighed. After introduction to the furnace, through the sample inlet device, 5 seconds elapsed before the sample was dropped into the crucible, so as to eliminate any air which could have been in the chamber. Frequent checks of electronic balance of the instrument, and recalibration every 5 to 10 samples provided a useful means of checking the proper behaviour of the instrument.

A few low carbon analyses were performed also on the LECO analyser. The procedure followed was the procedure recommended by the manufacturer.

CHAPTER III

Experimental Procedure

3.1 Gas train

3.1.1 $CO-CO_2$ gas train

The mixtures with analyses were obtained from the Matheson company. A few checks were made with an Orsat apparatus. The results were in good agreement. The gas was passed through magnesium perchlorate for removal of traces of moisture (Fig. 5).

Two stopcocks allowed the introduction of Helium or hydrogen to the reaction chamber, for fusion, cooling or deoxidation. The Helium purifying train was composed of ascarite (sodium hydroxide on asbestos support) for CO_2 removal and magnesium perchlorate for water vapor removal. The main impurity was hydrogen (< 20 p.p.m.). Hydrogen was passed over a palladium catalyst at room temperature, reducing the oxygen level to very low figures (< 1 p.p.m.), and over magnesium perchlorate for removing traces of moisture.

3.1.2 H_2 - H_2O,high and medium water vapor contents

The hydrogen water vapor mixtures of high and medium H_2O/H_2 ratios (greater than 3×10^{-2}) were produced with the aid of a constant temperature saturator. (Fig. 6). The hydrogen, or hydrogen-helium mixture was passed through a palladium catalyst at room temperature, and a presaturator maintained at a temperature slightly greater than the controlled temperature of the saturator. The saturator was composed of seven glass flasks filled with distilled water, and immersed in a water bath. The temperature was controlled by a resistance heater (manufactured by Gebruder Haake-Berlin) which maintained a constant circulation in the bath. The control was better than 0.1°C in the bath. The tubes leaving the saturator were heated with nichrome wire, maintained at about 80°C, in order to avoid any condensation.

The slight pressure drop in the line was measured by a dibutyl phtalate manometer, placed just after the saturator. The efficiency of this equipment was checked over a wide range of operating conditions. During the checks, the temperatures in the last saturator flask and in the water bath were measured with iron-constantan thermocouples and continuously recorded. The water vapor was absorbed by 4 tubes filled with magnesium perchlorate and previously weighed. The 4th tube was used as a check to ensure that all the water vapor was eliminated from the incoming gas. Its weight did not change during experiments. The amount of water was deduced by weight of the three other absorbing vessels. The volume of gas passed through was measured by a laboratory Wet Test Meter, previously calibrated for hydrogen with the soap bubble method. The only gas passed through the saturator was hydrogen.

The temperature of the bath was varied from 30 to 47°C. The flow rates covered the range 1000 - 6000 cc/minute . It was found that 15 to 30 minutes were necessary to attain thermal equilibrium inside the flasks (although the temperature of the bath was practically constant). Values of P_{H_2O}/P_{H_2} were within 1% of the theoretical values.

Appendix I is a calculation of the correction for non ideality at saturator temperature. This correction is negligible when compared to the experimental errors.

3.1.3 H_2-H_2O mixtures of low water vapor content

The low H_2O/H_2 ratios needed for obtaining oxygen potentials below the oxygen potential of oxide formation for high chromium alloys would have required water bath temperatures less than 10°C. This is rather awkward to control. Instead, solid oxalic acid dihydrate was used, at temperatures between 30 and 50°C. Baxter and Lansing(41) point out the possible use of various solid crystals for obtaining such low vapor pressures. They investigated the dissociation pressure of various hydrates. Oxalic acid dihydrate has been used by several authors since(42,43,44) and they all confirm the validity of Baxter's equation.

The gas train is schematically shown on Fig. 7. Hydrogen was passed over a palladium catalyst, then dried on magnesium perchlorate. Four U-tubes, 1.5 cm in diameter were filled with the mixture recommended by Baxter(41) and immersed in the water bath. A check of the efficiency was made with the same technique as in 3.1.2 at one temperature (48.9°C) and at a flow rate of hydrogen of 1 liter/min. The agreement with the data of Baxter is excellent and his equation was used subsequently.

3.2 Reaction chamber and quenching mechanism

3.2.1 Copper mold quenching

The reaction chamber with copper mold quenching can be seen in Fig. 8. Two different types of copper mold were used. The first one (Fig. 9) was used for oxygen levels below 0.08%. In this case the entire sample was used for oxygen analysis. A second type (Fig.10, a "split mold") was used for oxygen levels higher than 0.08%. The quenched sample obtained has a deep groove and is easily cut in two with a pair of pliers, without any loss of metal. The two halves were subsequently analysed for oxygen. When $CO-CO_2$ was used with pure iron or low chromium Fe-Cr alloys, a little piece of aluminum wire of high purity (99.9995% Al) was used for avoiding carbon boil when the sample was quenched. Pieces of aluminum of similar weight (placed in tin capsules) were analysed for oxygen but no trace was detected.

3.2.2 Piston and anvil quenching device

The reaction chamber and the piston and anvil device appear in Fig. 12, and 13. This fast quenching equipment was previously used by Gommersal(45). A slight modification was made by replacing the sliding brass contact with a microswitch. A sliding valve was attached to the top of the cylinder block, which provided a gas tight and easily heated base for the reaction chamber. Condensation was then avoided when H_2-H_2O was used. A thin plastic film separated the gas in the reaction chamber from the gas in the quenching system. This film (identical to the one used by Baker(46)) did not interfere with the free fall of the droplet. Helium was kept flowing through the cylinder, thus providing a slight surpressure to minimize any oxygen diffusion which might have reacted with the droplet during quenching.

All runs with numbers below 1200 were quenched with this apparatus. There is no statistical difference between these results and the results of Kershaw(40) made under the same conditions, but quenched in a copper mold.

3.3 Sample preparation

Armco iron was used in the form of rods, ¼ inch diameter. After removal of the superficial oxide layer, the rod was cut into samples of about 1g. The rough edges of the sample were removed on a sand grinder, the samples washed several times in acetone and stored until use in a dessicator.

Ferrovac E (analyses in Table III) was provided by United States Steel Corp. in the form of 1 inch bars. They were swaged down to ¼ inch rods and prepared in the same way as the armco.

The Fe-Cr alloys were made from ferrovac E and chromium of 99.95% purity. They were melted in an argon-arc furnace and cast into an elongated copper mold. The ingot was then swaged down to a rod of ¼ inch diameter. The procedure was then identical to that described above.

Samples from the ends and from the middle of each rod were analysed for chromium by the standard oxidation method. Within the precision of analyses (± 0.05%) no segregation was detected in the rod. The analyses are in good agreement with the theoretical composition, which indicates that no alloying element was lost during melting.

3.4 Experimental procedure

The specimen was first washed in acetone and dried, then introduced into the reaction chamber on top of a silica rod. The reaction chamber was flushed with helium. The flow was then reduced to a low value (around 500 cc min.$^{-1}$ or less), the power switched on and increased to its maximum value. The sample was lowered into the coil, and was levitated as soon as the Curie point was reached (less than a second). Melting took place very quickly. In view of the mechanical instability of the specimen around the melting point, and the possibilities for the sample to stick to the wall of the reaction tube, it is important to keep this process rapid.

Despite its good thermal conductivity, hydrogen was used in melting of iron-chromium alloys. Thus formation of oxide (which tended to make the sample spatter on melting) was avoided.

Helium was preferred to argon because:

i) the hydrogen content makes it reducing with respect to iron oxide.

ii) there is no steep and rapid rise of temperature after the specimen is molten.

Some of the samples were deoxidized for 4-5 minutes at 1600°C. The oxygen left after this treatment is not detectable with the oxygen analyser (less than 4 or 5 p.p.m.). Then the oxidizing gas was introduced. When H_2-H_2O was used, H_2 had been flowing through the saturator, at the flow rate chosen for the experiment (generally 1 liter/min.) for at least ½ an hour prior to the initial experiment.

Oxide generally appeared on the sample after 30 seconds to 1 minute of exposure. The movements of the particles showed the large agitation of the drop at the surface. This oxide however represented only a rapid surface concentration of oxygen. (As indicated by the low total oxygen content of samples quenched after 1 minute of exposure.) The particles generally disappeared after about 2 minutes. This phenomenon is discussed in more detail in the next paragraph.

3.5 Attainment of steady state

Fig. 14 summarizes the study of the kinetics of dissolution of oxygen from CO-CO_2 gas mixtures at 1550°C. The steady state is generally reached within 10 minutes. As a further precaution samples were held 15 minutes in the gas. These figures are of the order of magnitude of the figures of Richardson(39) for the dissolution of oxygen from $CO-CO_2$ gas mixtures in nickel.

The kineticsof dissolution of oxygen from H_2-H_2O gas mixtures is slightly faster. Runs 1101 to 1125 indicate that the steady state is reached within 5 minutes at 1600°C.

It was observed that the oxides appearing on Fe-Cr alloys, when the H_2-H_2O mixture is introduced, are more difficult to reduce than iron oxide. Therefore the experiments with these alloys were carried out over a longer period of time. It is interesting to note that the kinetics are very much lower at 1550 than at 1600°C.

CHAPTER IV

The Iron-Oxygen System

4.1 Dissolution of oxygen from H_2-H_2O mixtures

4.1.1 Introduction

The dissolution of oxygen from H_2-H_2O gas mixtures can be described by the reaction

$$H_2 + \underline{O} = H_2O$$

with the equilibrium constant

$$K_1 = \frac{P_{H_2O}}{P_{H_2} \times a_o}$$

and the pseudo equilibrium constant

$$K_1' = \frac{P_{H_2O}}{P_{H_2} \times (\% O)}$$

the relation between K_1 and K_1' being

$$\log K_1 = \log K_1' - \log f_o$$

The results which were first observed were markedly different from results of previous investigators (Fig. 15). A series of experiments was conducted in order to determine the causes of those discrepancies.

4.1.2 Experiments with Armco iron and ferrovac 'E'.

Armco iron contains 99.9 wt.pct. of iron. The mean oxygen level is about 0.07 pct, but in the present instance this is not considered as an impurity. Although the effect of the impurities present is small (Appendix II), experiments after 1122 were performed with ferrovac 'E'.

A statistical comparison between the results obtained at 1600°C with the two materials (runs 1023-1030 and 1123-1128) shows no difference. The test was a standard 'student t' test, at 95% confidence(47) (Appendix III).

4.1.3 Effect of gas flow rate with H_2-H_2O mixtures

The effect of flow rate can only be compared between runs 1158-1163 and runs 1123-1130. A 'Student t' test does not show any difference between the two sets of data. This is substantiated by the work of Kershaw(40), who did not find any effect of flow rate on the steady state values of log K_1'.

4.1.4 Effect of droplet size

Droplets of 1.4 to 0.6g were levitated in H_2-H_2O - He mixture at 1600°C. The surface to volume ratio, assuming a spherical shape for the drop, is given by

$$s/v = \frac{3}{\left(\frac{3}{4}\frac{m}{\pi\rho}\right)^{1/3}}$$

m and ρ being the mass and density of the sample respectively. Taking the value of ρ for pure iron at 1600°C as 7.16 g cm^{-3} (48) this ratio varied from 1105 to 832 cm^{-1}, i.e. a difference of about 25%.

Unfortunately it was impossible to maintain the same gas flow rate in both sets of experiments, because of temperature control.

A test comparing the two sets of data (as in 4.1.2 and 4.1.3) show, with a high degree of confidence ($t = 0.21$) that there is no difference between them.

A comparison of runs 1158 to 1163 and 1123 to 1130 with flow rates of respectively 400 to 500 cc $min.^{-1}$, and weight of .6 and 1.1 g. are also statistically the same. The oxygen level of the first series was slightly higher than oxygen level of the second, due to the use of H_2-H_2O-He mixtures instead of H_2-H_2O mixtures.

4.1.5 Experimental results

The results are compiled in Table V to X. A graphical summary appears in Fig. 15, along with results of previous investigators.

The effect of oxygen content on the pseudo-equilibrium constant K_1' was investigated but not measurable. No deviation from Henry's law was observed.

The main feature of the results is the discrepancy between the present data and those of recent investigators. The nature of this discrepancy suggests that thermal diffusion effects might be significant. In view of the large thermal gradient around the droplet and the nature of the gas mixture this would not be unexpected. To check this possibility the system was reinvestigated with CO-CO_2 gas mixtures which would not be as susceptible to thermal diffusion effects as H_2-H_2O gas mixtures.

4.2 Dissolution of oxygen from CO-CO_2 gas mixtures

4.2.1 Experimental results

The dissolution of oxygen from CO-CO_2 mixtures can be described by the reaction

$$CO + \underline{O} = CO_2 \tag{4.05}$$

with the equilibrium constant

$$K_2 = \frac{P_{CO_2}}{P_{CO} \times a_o}$$

and the pseudo-equilibrium constant

$$K_2' = \frac{P_{CO_2}}{P_{CO} \times (\%\ O)}$$

The variation of K_2' with oxygen content was studied at 1600°C with gas mixtures ranging from 0.5 to 15% CO_2. The effect of temperature on the equilibrium constant was investigated from 1550°C to 1750°C, using a gas mixture of 5.34% CO_2.

The results are compiled on Tables XI to XIII. The effect of oxygen content and the effect of temperature are summarized graphically on Fig. 16 and 17.

The effect of oxygen content on log K_2' was treated by the least mean square method. However no significant deviation from Henry's law was observed. Using the value of Floridis and Chipman$^{(21)}$ for the self interaction parameter of oxygen, at 1600°C

$$e_o^{(o)} = -0.20$$

this would give a difference between log K_2 and log K_2' of 0.03 units at the highest oxygen level, and 0.004 at the lowest oxygen level. This is certainly within the range of errors due to oxygen analysis, particularly for droplets with high oxygen content which have been analyzed with samples cut into 2, 3 or even 4 parts.

The oxygen levels obtained with gas mixtures of 5.34% CO_2, at 1600°C, are of the order of 0.05 - 0.06 wt. pct. The error involved by assimulating log K_2' and log K_2 would be of the order of 0.01. This effect is easily covered by errors in oxygen analyses and it is therefore neglected in the interpretation of the temperature dependant data.

The effect of temperature is shown on Fig. 17. The least mean square straight line yields the equation

$$\log K_2 = -4.519 \ (\pm 0.095) + \frac{8421}{T} \ (\pm 939) \qquad (4.09)$$

The corresponding free energy change for the reaction is

$$\Delta G^{o} = - 38530 + 20.67/T \qquad (4.1)$$

4.2.2 Thermodynamic calculations

The Fe-O system has been investigated most frequently with H_2-H_2O mixtures. It is therefore convenient for comparison purposes, to calculate a value of log K_1 from equations (4.09) and (4.1). From the thermodynamic expression

$$RT \ln K = - \Delta G^{o} \qquad (4.2)$$

or

$$4.575T \log K = - \Delta G^{o} \qquad (4.3)$$

and the free energy change for the water gas reaction (ref. 51)

$$H_2\ (g) + CO_2\ (g) = H_2O\ (g) + CO\ (g) \qquad (4.4)$$

$$\Delta G^{o} = 6355 - 6.24\ T$$

the free energy change for the reaction

$$H_2 + \underline{O} = H_2O \qquad (4.5)$$

was found to be

$$\Delta G^{o} = - 32270 + 14.45\ T$$

and therefore

$$\log K_1 = 7054/T - 3.158$$

From the standard expression

$$\Delta G^{o} = \Delta H^{o} - T\Delta S^{o}$$

assuming that ΔH^{o} and ΔS^{o} are constant with temperature over the range of interest, then for the reaction

$$CO + \underline{O} = CO_2$$

$$\Delta H^o = -\ 38530 \text{ cal.}$$

$$\Delta S^o = -\ 20.67 \text{ e.u.}$$

and for the reaction

$$H_2 + \underline{O} = H_2O$$

$$\Delta H^o = -\ 32270$$

$$\Delta S^o = -\ 14.45$$

Finally, using the reaction:

$$H_2(g) + \tfrac{1}{2}\,O_2\ (g) = H_2O\ (g)$$

with the free energy change:

$$\Delta G^o = -\ 60200 + 13.94T \qquad \text{(ref.51)}$$

the free energy, enthalpy and entropy change for the dissolution of oxygen in liquid iron

$$\tfrac{1}{2}\,O_2\ (g) = \underline{O}\ (1 \text{ wt. pct.})$$

are:

$$\Delta G^o = -\ 27930 - 0.51\ T$$

$$\Delta H^o = -\ 27930 \text{ cal.}$$

$$\Delta S^o = 0.51 \text{ e.u.}$$

4.2.3 Comparison with previous studies

The results of the investigation with CO-CO_2 are compared with other workers who used the same gases in Table XIV and Fig. 18, and with studies using H_2-H_2O in Table XV and Fig. 15.

The results are in good agreement with Dastur and Chipman(20) and Floridis and Chipman(21); and in reasonable agreement with Sakao and Sano(10).

This is a confirmation that thermal diffusion effects are within the limits of experimental uncertainties when CO-CO_2 gas mixtures are used to control the oxygen potential of the gas phase during levitation melting experiments of the type described in this investigation. However it should be noted that thermal diffusion effects are significant when H_2-H_2O gas mixtures are used under the same conditions.

It is worthwhile to point out that values for the free energy change for the water gas reaction are not in complete agreement. This introduces some uncertainty, when comparing these data with data obtained with H_2-H_2O gas mixtures. ($\pm$ 1.5 kcal on ΔG^o).

2.4 Discussion

When CO-CO_2 gas mixtures are used, a second reaction can occur:

$$CO_2 + \underline{C} = 2CO$$

In other words, the system of interest is now ternary in nature: Fe-O-C. A few droplets, levitated at 1600^oC for 5 minutes, in a mixture containing 5.34% CO_2, were analysed for carbon. (The method used was described in Section 2.4). The results are shown below:

Sample N^o	wt. pct. C.
1294	0.046
1295	0.031
1296	0.031
1297	0.037

The effect of a concentration of 0.04 wt. pct. C on the oxygen content of a sample can be calculated as follows:

Assuming e_O^O is zero, the activity coefficient of oxygen, in the presence of carbon is

$$\log f_O = e_O^C (\% C)$$

from ref. 51, $e_O^C = 0.13$. Therefore

$$\log f_O = 0.0052$$

The change introduced in log K' by the presence of carbon is well within the experimental precision of the data and can therefore be neglected.

It is interesting to note that the values found for the concentration of carbon are in reasonable agreement with the equilibrium values of Rist$^{(52)}$. Using Rist's data, and taking the total gas pressure as 1 atm., the equilibrium concentration of carbon should be 0.03 wt. pct. It can be assumed therefore, that the carbon in the melt is in equilibrium with the gaseous phase. The amount of carbon dissolved for all gas mixtures of higher carbon dioxide concentration is then lower than 0.04 wt. pct. and the effect is negligible.

The gas mixture of lowest carbon dioxide content has a composition of 1.99% of CO_2. The carbon dissolved at equilibrium with this gas, assuming a total pressure of 1 atmosphere would be approximately 0.8 wt. pct. The effect on log K is 0.09. In view of the dispersion of the data at this oxygen level, this effect was not taken into account.

Other errors, which would explain the distribution of the results, can be attributed to the various sources discussed already in Chapter II and III.

CHAPTER V

Effect of Chromium on the Solubility of Oxygen in Liquid Iron

5.1 Experiments conducted with $CO-CO_2$ mixtures

5.1.1 Introduction

When oxygen dissolves in liquid iron-chromium alloys exposed to $CO-CO_2$ gas mixtures, the following reaction occurs:

$$CO + \underline{O} = CO_2$$

and the equilibrium constant K_2 is given by:

$$K_2 = \frac{P_{CO_2}}{P_{CO} \times (f_o \times \%\ O)}$$

where f_o is the activity coefficient of oxygen in the solution. As shown in Chapter I, f_o can be mathematically represented by an expression of the form:

$$\log f_o = e_o^{(o)} \times (\%\ O) + e_o^{(Cr)} \times (\%\ Cr) + r_o^{(o)} \times (\%\ O)^2 + r_o^{(Cr)} \times (\%\ Cr)^2$$
$$+ r_o^{(Cr,O)} \times (\%\ Cr) \times (\%\ O) + \ldots \qquad (5.1)$$

In the present work, the oxygen level is considered sufficiently low that terms involving $e_o^{(o)}$ and $r_o^{(o)}$ can be neglected. $r_o^{(Cr,\ O)}$ cannot be determined directly from the data gathered since no experiments were made at constant chromium content, and various oxygen potentials. It was thus assumed that the product $r_o^{(Cr,\ O)}$ (% Cr) x (% O) was negligible in comparison with r_o^{Cr} $(\%\ Cr)^2$. This means that, with an alloy with 25% Cr, and an oxygen level of less than 0.02, the term $r_o^{(Cr,O)} \times 0.5$ is negligible in comparison with r_o^{Cr} x 625, i.e. that $r_o^{(Cr,O)}$ is less than 10 to 100 times larger than $r_o^{(Cr)}$. This seems a reasonable assumption in view of the empirical formula$^{(5)}$

$$\rho_i^{(j,i)} = \rho_i^{(j)} + \rho_i^{(i)}$$

which may provide a reasonable estimate of the cross-product interaction coefficients.

With these simplifications, equations (5.1) becomes

$$\log f_o = e_o^{(Cr)} (\% \ Cr) + r_o^{(Cr)} (\% \ Cr)^2$$

The two interaction parameters can be determined from a plot of log $[P_{CO_2}/P_{CO}$ x (% O)] versus wt. percent chromium.

5.1.2 Experimental results

The results of the investigation with CO-CO_2 gas mixtures at 1600°C and chromium contents up to 10 wt. pct. are contained in Table XVI and shown in Fig 19. The data were treated statistically by the least mean square method. This treatment yields the following equation

$$\log f_o = - 0.058 (\% \ Cr) + 1.25 \times 10^{-3} (\% \ Cr)^2$$

In view of the relatively low range of concentrations considered in this series of experiments (0 - 10% Cr), the uncertainty associated with the second order parameter is greater than that associated with the first order term. A check on the effect of carbon dissolution on these data was shown to be negligible (Appendix IV).

5.2 Experiments conducted with H_2-H_2O mixtures

5.2.1 Introduction

It is experimentally more difficult to obtain data using gas mixtures of CO-CO_2 rather than H_2-H_2O with levitation melting, due to problems of temperature control and low oxygen potentials. However, CO-CO_2 gas mixtures are not strongly affected by thermal diffusion. It was therefore planned to use the interaction coefficients obtained with CO-CO_2 as a check on the validity of the interaction coefficients obtained with H_2-H_2O at the same temperature.

The treatment is similar to the one used in Section 1.1. The reaction under consideration is:

$$H_2 + \underline{O} = H_2O$$

and the equilibrium constant is given by:

$$K_1 = \frac{(P_{H_2O})}{P_{H_2} \times (f_o \times \%\ O)}$$

5.2.2 Experimental results

The results of experiments with iron-chromium alloys up to 25 wt.pct. and temperatures in the range of 1550°C to 1750°C are collected in Tables XVII to XXI and figs. 20 to 24. The statistical treatment used was a least mean square fitting to a parabola. The first and second order interaction coefficients are shown below

Temperature °C	$e_o^{(Cr)}$	$r_o^{Cr} \times 10^4$
1550	-0.068	10.6
1600	-0.059	6.8
1650	-0.051	6.0
1700	-0.037	1.6
1750	-0.041	4.6

A fitting to a polynomial of the third degree was tried. The first and second order terms thus obtained are generally in good agreement with the previously derived data. This constitutes a check of the relatively low scatter of the data, the agreement increasing with decreasing dispersion.

A plot of the interaction parameters versus the reciprocal of the absolute temperature (Fig. 26) shows a decrease of the chromium-oxygen interaction with increasing temperature. The statistical straight lines have been calculated as:

$$e_o^{(Cr)} = - 563.4/T + 0.242$$

$$r_o^{(Cr)} = 12.86/T - 6.10 \times 10^{-3}$$

Using the notations of Lupis and Elliott$^{(5)}$ these equations can be expressed in terms of entropy and enthalpy interaction parameters. The following table gives these values:

Parameter Function	First order	Second order
Enthalpy	$h_o^{(Cr)} = - 2578$	$l_o^{(Cr)} = 58.83$
Entropy	$s_o^{(Cr)} = - 1.107$	$p_o^{(Cr)} = 2.79 \times 10^{-2}$

The values for these coefficients on the mole fraction scale are given in Table 23. The logarithm of the activity coefficient of oxygen in liquid iron-chromium alloys in terms of temperature and chromium concentration is given by

$$\log f_o = (-563.4/T + 0.242) \times (\%\ Cr) + (12.86/T - 6.10 \times 10^{-3}) (\%\ Cr)^2 \quad (5.2)$$

Chipman and Corrigan$^{(56)}$ found a linear relationship between first order free energy and enthalpy interaction parameters. This has later been explained, on the basis of a statistical model of solution, by Lupis and Elliott(57). It seems to be of interest for estimating the effects of different solutes on the same solvent-solute interaction (system 1-2-i). In order to help in the determination of this constant for the Fe-O-j system, this parameter has been determined in our case. The relation is given by:

$$\frac{\varepsilon_2^i}{\eta_2^i} = \frac{1}{R} \left(\frac{1}{T} - \frac{1}{\tau}\right) \text{ (ref. 57)}$$

The value obtained for τ is:

$$\tau = 2925^{\circ}K .$$

5.2.3 Comparison with previous investigations

Table II summarizes the results available on chromium-oxygen interactions. Only first order free energy interaction parameters have been determined so far. It was generally assumed that the variation of this parameter with temperature was small.

At 1600°C, the agreement is very good with McLean and Bell(8), and with Turkdogan(7). However, it is significantly lower than the value found by Chen and Chipman(6,9).

5.2.4 Comparison between $CO-CO_2$ and $H_2 - H_2O$ data

Good agreement exists between the two sets of data. Because of the relatively smaller range of chromium used with the $CO-CO_2$ gas mixtures, the comparison of the first order free energy interaction parameter is more significant.

The similarity between the two sets of data shows clearly that thermal diffusion does not significantly affect the values obtained for relative effects such as the effect of an alloying element on oxygen activity. Thus levitation melting can be used with H_2-H_2O gas mixtures for determining the effects of alloying elements on the behaviour of oxygen. This technique is particularly suited for obtaining data at temperatures above 1700°C without interference from crucible material.

5.2.5 Chromium-oxygen relationships in liquid iron in equilibrium with Cr_3O_4

The equilibrium of dissolved oxygen and chromium in liquid iron with Cr_3O_4 can be described by the equation:

$$Cr_3O_4(s) = 3\,\underline{Cr} + 4\,\underline{O}$$

with the equilibrium constant

$$K_3 = \frac{(a_{Cr})^3\,(a_O)^4}{a_{Cr_3O_4}}$$

Taking the standard state for Cr_3O_4 as pure substance, $a_{Cr_3O_4} = 1$, we can write

$$\log K_3 = 3 \log a_{Cr} + 4 \log a_O \qquad (5.3)$$

The Fe-Cr solution is nearly ideal$^{(53)}$ and $e_{Cr}^{(O)}(\%\ O)$ was considered to be negligible. Therefore 5.3 can be rewritten as:

$$\log K_3 = 3 \log (\%\ Cr) + 4 \log a_O \qquad (5.4)$$

A log - log plot of a_O versus % Cr should give a straight line. Using the interaction parameters previously determined, one can show on the same graph

(Fig. 28) the relation between log (% O) and log (% Cr).

The value of K_3 has not been established; however Chipman's estimation of ΔG^o for the reaction 5.3 is:

$$\Delta G^o = 250000 - 109.4T$$

This yields

$$\log K_3 = \frac{-54645}{T} + 23.91$$

Cr_3O_4 being the oxide present when the amount of chromium is greater than approximately 10%, (54) the plot was constructed for the range 10-25%. It was calculated on the basis of the same interaction coefficients up to 40 wt. pct. Cr. On the same graph, the dotted lines indicate the amount of oxygen present, calculated if only first order effects are taken into account. The discrepancy increases with increasing chromium concentration and decreasing temperature.

In addition, the calculated oxygen level in equilibrium with the oxide is continuously increasing with chromium content, when first order parameters only are used. Under certain circumstances second order effects can introduce a maximum point in additon to the minimum point generally observed in curves of this nature. This might explain the somewhat strange results obtained by d'Entremont et al(55) when studing aluminum-oxygen relationship in liquid iron in equilibrium with alumina at high aluminum concentrations. (cf. appendix 6)

It would be interesting to study the equilibrium of molten iron with Cr_3O_4 at high chromium levels, in order to test the validity of the second order interaction parameter determined in this study.

5.2.6 Discussion

The accuracy of the measurements of the controlled variables and their influence on the precision of the final results have been already discussed in connection with experimental apparatus and techniques. The estimated errors involved with the various measurements are summarized below:

i) ± 10°C in the measurement and control of the temperature of the droplet;

ii) ± 0.1°C in the measurement of water bath temperature;

iii) 0.5 to 1% error in saturator efficiency;

iv) ± 5 to 10 p.p.m. uncertainty in oxygen analyses;

v) 1 to 2% uncertainty in chromium content of the Fe-Cr alloys;

vi) approximately 1% on the CO_2 percentage of CO-CO_2 mixture.

The errors involved in pressure measurements have an effect which is far smaller, on log K' values, than the previously cited sources of errors.

Crucible techniques are also susceptible to errors of the same nature. It seems however, that the scatter of data obtained by levitation melting is sometimes slightly larger than with data secured with other methods. This may be accounted for by the sometimes unstable mechanical behaviour of the droplet. This makes precise temperature control more difficult. If the reaction kinetics are not slow enough for smoothing out these fluctuations, they can be reflected in the final oxygen content. The easier control obtained with H_2-H_2O mixtures favored its use instead of CO-CO_2 as an oxygen potential controlling mixture. The relative ease with which data are obtained with levitation melting techniques also allows the average dispersion to be statistically reduced.

The various assumptions made when using levitation melting are:

i) There is no significant temperature gradient inside the droplet, and its surface temperature is a good representation of its mean temperature;

ii) There is a sufficiently good stirring inside the drop, to insure homogeneity of composition.

It has been shown that, within the limits of experimental scatter:

i) The steady state is attained within 5 to 15 minutes depending on temperature and the nature of the gas mixture;

ii) Surface effects are too small to interfere with data representative of the bulk composition;

iii) Gas flow rates from 400 to 4000 cc/minute, with gas mixtures subject to thermal diffusion, do not affect the steady state, insofar as oxygen dissolution is concerned;

iv) Surface stirring is vigorous, as indicated by the movement of occasional oxide particles.

The evaporation of chromium during experiments has been checked. Two samples containing 14.6 wt.pct chromium have been levitated in hydrogen, at 1700°C during 15 and 20 minutes. The final chromium content was 14.1 and 14.0 wt. pct.

In conclusion, with the type of levitation melting equipment used in this investigation:

i) H_2-H_2O gas mixtures are subject to thermal diffusion effects;

ii) The effects of thermal diffusion on oxygen dissolution from

CO-CO_2 mixtures are negligible.

ii) The values obtained for chromium-oxygen interaction parameters using both types of gas mixtures are in good agreement.

SUMMARY

The solubility of oxygen in liquid iron, has been investigated with H_2-H_2O and CO-CO_2 gas mixtures, over the temperature range 1550°C to 1750°C. H_2-H_2O mixtures are subject to thermal diffusion effects and cannot be used for the determination of equilibrium constants. However, CO-CO_2 mixtures can be used for this purpose and the values obtained for the reaction:-

$$CO + \underline{O} = CO_2 \quad ,$$

are given by the expression:-

$$\log K_2 = 8421 \; /T \; - 4.519$$

The effect of chromium on the behaviour of oxygen dissolved in liquid iron has also been studied. This effect can be represented by the equation

$$\log f_0 = (-563.4/T + 0.242) \times (\% \text{ Cr}) + (12.86/T - 6.8 \times 10^{-3}) \times (\% \text{ Cr})^2$$

Although thermal diffusion effects influence the dissolution in liquid iron of oxygen from H_2-H_2O mixtures, these gases can be used for determination of interaction coefficients. The values are in agreement with those obtained with CO-CO_2 mixtures, in which thermal diffusion effects do not significantly influence the transfer of oxygen from the gas phase into the melt.

The effect of a second order interaction coefficient on the amount of oxygen in equilibrium with chromium dissolved in liquid iron and solid Cr_3O_4 has been calculated, and compared with the values obtained when using only a first order interaction parameter.

APPENDIX I

Correction of the ratio $\frac{P_{H_2O}}{P_{H_2}}$ for non ideality of the gas mixture

The problem is to calculate the ratio

$$K\ (T) = \frac{f_{H_2O}}{f_{H_2}} \tag{1}$$

f_{H_2O} and f_{H_2} being the fugacities of water vapor and hydrogen respectively at temperature T. No measured thermodynamic data were found for this gas mixture. It is therefore necessary to use a model to predict its behaviour.

If we represent the behaviour of the gas mixture by a power serie expansion

$$\frac{P}{kT} = \rho_1 + \rho_2 + B_{20}\ (T)\rho_1^2 + B_{11}\ (T)\ \rho_1\ \rho_2 + B_{02}\ (T)\ \rho_2^2 + \ .. \tag{2}$$

P	pressure of the mixture
k	Boltzman's constant
T	absolute temperature
ρ_1	molal density of component 1
ρ_2	molal density of component 2
B_{20}, B_{11}, B_{02}	virial coefficients

it can be shown (ref. 58)

a) B_{20} and B_{02} are the second virial coefficients for the pure gases 1 and 2

b) the fugacity has the expression

$$\frac{f_1}{kT} = \rho_1 + 2\, B_{20}\, \rho_1^2 + B_{11}\, \rho_1\, \rho_2 + \ldots \tag{3}$$

$$\frac{f_2}{kT} = \rho_2 + 2\, B_{02}\, \rho_2^2 + B_{11}\, \rho_1\, \rho_2 + \ldots \tag{4}$$

Replacing this value in (1) we found an expression for K (T)

$$K\,(T) = \frac{\rho_1\,(1 + 2\, B_{20}\rho_1 + b_{11}\, \rho_2 + ..)}{\rho_2\,(1 + 2\, B_{02}\, \rho_2 + B_{11}\, \rho_1 + ..)} \tag{5}$$

which, by dividing the two power series becomes:

$$K(T) = \frac{\rho_1}{\rho_2} [\; 1 + \rho_1\,(2\, B_{20} - B_{11}) + \rho_2\,(B_{11} - 2\, B_{02}) + ..\;] \tag{6}$$

B_{20} and B_{02} can be obtained from the Van der Waals equation for the pure gases.

$$(\, P + \frac{n^2 a}{V^2}\,)\,(V - nb) = n\, RT \tag{7}$$

which can be rewritten under the form

$$\frac{P}{kT} = \rho + \beta\, \rho^2 + \gamma\, \rho^3 + \ldots \tag{8}$$

with (ref 58)

$$\beta = b - \frac{a}{kT} \tag{9}$$

If we neglect γ and higher order terms in (8) and (2) we can write for the pure components 1 and 2, and the mixture

$$\frac{P_1}{kT} = \rho_1 + B_{20}\,(T)\, \rho_1^2 \tag{10}$$

$$\frac{P_2}{kT} = \rho_2 + B_{02}\ (T)\ \rho_2^2 \tag{11}$$

$$\frac{P}{kT} = \rho_1 + \rho_2 + B_{20}\ (T)\ \rho_1^2 + B_{02}\ (T)\ \rho_2^2 \tag{12}$$

The comparison of (10), (11) and (12) give:

$$P = P_1 + P_2 \tag{13}$$

in other words Dalton's law on partial pressures is applicable. Making the further assumption that B_{20} and B_{02} are almost constant over the temperature range 25-1750°C, the ratio $\frac{P_1}{P_2}$ remain constant with temperature.

This allows one to calculate the partial pressure of H_2 and H_2O at the temperature of the molten iron droplet.

No data are available on B_{11}, which is a measure of the interaction between two molecules of species 1 and 2. We will make an assumption similar to the assumption of ideal solutions, i.e. $B_{11} = 0$. We are now able to calculate the first order correction on K (T).

The numerical values for the Van der Waals constant are (ref. 59)

for H_2O

$$a = 5.434\ \frac{l^2 \times atm}{(moles)^2}$$

$$b = 0.0304\ l/mole$$

for H_2

$$a = 0.2444\ \frac{l^2 \times atm}{(moles)^2}$$

$$b = 0.02661\ l/mole$$

The calculation at $T = 1873^{0}K$ gives

$$\frac{\rho_1}{\rho_2} = \frac{P_1}{P_2} \quad \text{at a very good approximation}$$

and $K(T) = \frac{P_1}{P_2} [1 - 3 \times 10^{-4}]$

Therefore the correction on $\ln K_1$ is

$$\ln K_{1\text{corrected}} = \ln K_1 [1 - 3 \times 10^{-4}]$$

$$\simeq \ln K_1 - 3 \times 10^{-4}$$

This is negligible in comparison with the experimental errors on $\ln K_1$.

APPENDIX 2

Effect of impurities of Armco iron on oxygen dissolution.

The dissolution of oxygen from H_2-H_2O mixture is described by

$$H_2 + \underline{O} = H_2O$$

with

$$K_1 = \frac{P_{H_2O}}{P_{H_2} \times f_o \times (\% \ O)}$$

If the iron is not pure, f_o can be represented by:

$$\log f_o = \sum_i e_o^{(i)} (\% \ i) \qquad (1)$$

In the case of Armco iron it can be assumed that the solution is dilute. Neglecting oxygen self interaction, equation (1) becomes:-

$$\log f_o = e_o^{(c)} (\% \ C) + e_o^{(Mn)} (\% \ Mn) + e_o^{(P)} (\% \ P) \qquad (2)$$

$$+ e_o^{(s)} (\% \ S) + e_o^{(Si)} (\% \ Si) + e_o^{(Cu)} \% \ Cu$$

The values for the interaction parameters are taken from ref. 51. With the compositon listed in Table 3, this gives

$$\log f_o = - 0.004$$

The effect of this value on log K_1 is well within the limits of uncertainty discussed in detail in the text.

APPENDIX 3

Student 't' test

A standard student 't' test, for comparison of data n^o1023 - 1030 and no. 1123 - 1128 is described as an example.

The first population contains N_1 observations, and the second N_2, with means m_1 and m_2 and standard deviation S_1 and S_2. The variance of the total population is given by:-

$$r = \frac{N_1 \; S_1{}^2 + N_2 \; S_2{}^2}{N_1 + N_2 - 2}$$

$m_1 = 0.723$ $S_1^2 = 0.0017$

$m_2 = 0.725$ $S_2^2 = 0.0026$

The value of t is

$$t = \frac{m_1 - m_2}{r \; \frac{1}{N_1} + \frac{1}{N_2}}$$

$$= 0.21$$

The value for t, at the 5% level is 2.23. It can be concluded that there is no difference, at this level, between the populations.

APPENDIX 4

Effect of carbon dissolution on the Fe-O-Cr equilibrium

When $CO\text{-}CO_2$ gas mixtures are used for controlling the oxygen potential of the gas phase at high temperature, the following two reactions occur:

$$CO + \underline{O} = CO_2 \qquad (1)$$

$$K_2 = \frac{P_{CO_2}}{P_{CO} \times a_o}$$

$$\underline{C} + CO_2 = 2CO \qquad (2)$$

$$K_3 = \frac{(P_{CO})^2}{P_{CO_2} \times a_c}$$

The activity coefficients of oxygen and carbon dissolved in Fe-Cr alloys are represented by:

$$\log f_o = e_o^{(O)} \times (\%\ O) + e_o^{(c)}\ (\%\ C) + e_o^{(Cr)} \times (\%\ Cr) \quad (3)$$

$$\log f_c = e_c^{(c)} \times (\%\ C) + e_c^{(O)}\ (\%\ O) + e_c^{(Cr)}\ (\%\ Cr) \quad (4)$$

where second order effects are neglected.

If during the study of reaction (1) the effect of carbon is neglected, the error introduced in $\log f_o$ is equivalent to $e_o^{(C)} x\ (\%\ C)$. Taking the value of K_2 obtained in the present study together with Rist's value$^{(52)}$ for K_3, (% O) can be eliminated between (1), (2), (3) and (4) and the final equation solved for (% C). The final equation is

$$e_o^{(C)} x\ (\%\ C) = \log K_2 - \log \frac{P_{CO_2}}{P_{CO}} + \log \left[\frac{-a}{e_c^{(O)}}\right] - e_c^{(O)}\ \frac{a}{e_c^{o}} \qquad (5)$$

with

$$a = \log K_3 - \log \frac{(P_{CO})^2}{P_{CO_2}} + \log (\%\ C) + e_c^{(C)} \times (\%\ C) + e_o^{(Cr)} (\%\ Cr)$$

This equation was solved for the various gas mixtures and Cr alloys used. The interaction parameters were taken from ref. 51. A test was also made on the influence of this parameter on the solution of equation (5). The results are listed below:

Parameters for every calculation:

$e_o^{(c)} = -0.130$ $e_c^{(Cr)} = 0.024$ $e_c^{(0)} = -0.097$

Variable parameters: 1) $e_o^{(0)} = 0.0$ $e_c^{(c)} = 0.22$

Cr wt pct	Correction on log K_2
2.02	- 0.011
3.92	- 0.003
9.99	- 0.001

2) $e_o^{(0)} = 0.0$ $e_c^{(c)} = 0.400$

Cr wt pct	Correction on log K_2
2.02	- 0.012
3.92	- 0.002
9.99	- 0.001

3) $e_o^{(0)} = 0.20$ $e_c^{(c)} = 0.22$

Cr wt pct	Correction on log K_2
2.02	- 0.006
3.92	- 0.005
9.99	- 0.017

The errors involved by neglecting the presence of carbon is well within the average dispersion of the data.

APPENDIX 5

Correction of $\frac{P_{H_2O}}{P_{H_2}}$ ratio due to dissociation of H_2O

Suppose we start from a mixture H_2, H_2O

n'_{H_2}, n'_{H_2O} = number of moles. Temperature T', Pressure P' we bring this mixture to Temperature T.

The partial pressures are P_{H_2}, P_{H_2O}, P_{O_2}

The number of moles n_{H_2}, n_{H_2O}, n_{O_2}

The temperature is T, the pressure P.

Assuming perfect gases at this temperature, we have the relations:

$$1)\quad P_{H_2} = \frac{RT}{V}\, n_{H_2}$$

$$2)\quad P_{H_2} = \frac{RT}{V}\, n_{H_2O}$$

$$3)\quad P_{O_2} = \frac{RT}{V}\, n_{O_2}$$

$$4)\quad P_{H_2} + P_{H_2O} + P_{O_2} = P$$

The oxygen and the hydrogen balances give:

$$5)\quad n_{H_2} + n_{H_2O} = n'_{H_2} + n'_{H_2O}$$

$$6)\quad \tfrac{1}{2}\, n_{O_2} + n_{H_2O} = n'_{H_2O}$$

Finally, the equilibrium constant for the reaction

$$H_2(g) + \tfrac{1}{2}\, O_2\ (g) = H_2O\ (g)$$

is

$$\frac{P_{H_2O}}{P_{H_2}\sqrt{P_{O_2}}} = a \tag{7}$$

Eliminating $\frac{RT}{V}$ between (1) (2) and (3), we obtain the system

$$\frac{P_{H_2O}}{P_{H_2}} = \frac{n_{H_2O}}{n_{H_2}} \tag{8}$$

$$\frac{P_{O_2}}{P_{H_2O}} = \frac{n_{O_2}}{n_{H_2O}} \tag{9}$$

from (5) and (6)

$$\frac{n_{H_2} + n_{H_2O}}{\frac{1}{2}\, n_{O_2} + n_{H_2O}} = 1 + \frac{n'_{H_2O}}{n_{H_2}}$$

which, combined with (8) and (9) gives:

$$1 + \frac{P_{H_2O}}{P_{H_2}} = (1 + \frac{n'_{H_2O}}{n'_{H_2}})\ (\frac{1}{2}\,\frac{P_{O_2}}{P_{H_2}} + \frac{P_{H_2O}}{P_{H_2}})$$

Or

$$1 + \frac{P_{H_2}}{P_{H_2O}} = (1 + \frac{n'_{H_2}}{n'_{H_2O}})\ (1 + \frac{1}{2}\,\frac{P_{O_2}}{P_{H_2O}}) \tag{10}$$

from (7)

$$P_{O_2} = \frac{1}{a^2}\ (\frac{P_{H_2O}}{P_{H_2}})^2$$

and

$$\frac{P_{O_2}}{P_{H_2O}} = \frac{1}{2}\ (\frac{P_{H_2O}}{P_{H_2}})\ \frac{1}{P_{H_2}} \tag{11}$$

The dissociation being small, if $K = \frac{P_{H_2}}{P_{H_2O}}$,

we have

$$1 + K = (1 + K')\left(1 + \frac{1}{2 \times a^2 P_{H_2} K}\right)$$

but

$$\frac{K'}{K} \simeq 1$$

$$P_{H_2} \simeq P'_{H_2O}$$

Therefore the correction is:

$$K \simeq K' + \frac{K'}{K \times 2 \times a^2 P_{H_2}}$$

$$K \simeq K' + \frac{1}{2 \times a^2 \times P'_{H_2}}$$

Numerical application:

$P'_{H_2O} = 40$ mm Hg

$P'_{H_2} = 720$ mm Hg

$a = 7690$ (log $a = 3.886$ at 1900°K, from JANAF thermochemical data, (ref. 57)

$$K' \simeq \frac{P'_{H_2}}{P'_{H_2O}}$$

$$\simeq \frac{720}{40} = 18.0$$

Correction: $\frac{1}{2 \times 5.91 \times 0.947 \times 10^7} \simeq 9 \times 10^{-9}$

This correction is perfectly negligible.

APPENDIX 6

Second order effect in equilibrium reactions between molten Fe-O-j alloy and the corresponding oxides.

The equilibrium between an oxide and its components dissolved in molten iron can be represented by the reaction

$$M_mO = m\,\underline{M} + \underline{O} \tag{1}$$

$$K = \frac{a_o\,(a_M)^m}{a_{M_mO}} \tag{2}$$

If the oxide is pure, the logarithm of equation (2) becomes

$$\ln K = \ln a_o + m \ln a_m \tag{3}$$

A log - log plot of the activity of oxygen versus X_M gives a straight line when the Fe-M solution is ideal, a curve when the solution is not ideal. It is of interest to investigate the shape of the oxygen content versus X_M curve on the same plot, for the case when the second order effect of M on oxygen is not negligible. This is represented mathematically by:

$$\log f_o = \varepsilon_o^{(o)}\ X_o + \varepsilon_o^{(M)}\ X_M + \rho_o^M\ X_M^2 \tag{4}$$

$$\log f_M = \varepsilon_M^{(M)}\ X_M + \varepsilon_M^{(o)}\ X_o + \rho_M^{(o)}\ X_o^2 \tag{5}$$

If the oxide is more stable than iron oxide and X_o is small, then $\varepsilon_M^{(o)}\ X_o$,

$\rho_M^{(o)}$ $X_o^{\,2}$ and $\varepsilon_o^{(o)}$ X_o can be neglected.

Expression (4) becomes:

$$\ln K = \ln(X_o) + m\ \ln(X_M) + (\varepsilon_o^{(M)} + m\,\varepsilon_M^{(M)})\ X_M + \rho_o^{(M)}\ X_M^{\,2} \tag{6}$$

Using the following notation

$$x = \ln\ (X_M)$$

$$y = \ln\ (X_o) \tag{7}$$

(6) becomes:

$$y = \ln\ K - m\ x - (\varepsilon_o^{(M)} + m\ \varepsilon_m^{(M)})\ e^x - \rho_o^{(M)}\ e^{2x} \tag{8}$$

The extreme points of this curve will be investigated as functions of $(\varepsilon_o^{(M)} + m\,\varepsilon_M^{(M)}) =$ a and $\rho_o^{(M)}$, when x varies from $-\infty$ to o.

The derivatives of (8) with respect to x, gives

$$y' = -\ m - a\ e^x - 2\rho_o^{(M)}\ e^{2x}$$

$$y'' = -\ a\ e^x - 4\rho_o^{(M)}\ e^{2x}$$

$$= -\ e^x\ (a + 4\rho_o^{(M)}\ e^{\ x})$$

Notation:

$$y_1' = a + 4\rho_o^{(M)}\ e^{\ x}$$

With the deoxidizers generally used, $\varepsilon_o^{(M)} < o$, and one would expect $\rho_o^{(M)}$ to be positive. $m\,\varepsilon_M^{(M)}$ may be positive or negative. Thus y_1' is positive over the interval $(-\infty, o)$ and y_1 is increasing.

The extreme values are

$$y_1\ (-\infty) = \varepsilon_o^{(M)} + m\ \varepsilon_M^{(M)}$$

$$y_1(o) = \varepsilon_o^{(M)} + m\,\varepsilon_M^{(M)} + 4\rho_o^{(M)}$$

Case a

$$\varepsilon_o^{(M)} + m\,\varepsilon_M^{(M)} + 4\rho_o^{(M)} < 0$$

In this case y_1 is always negative, and, because $- e^x$ is always negative, y" is always positive. Then over the range $(-\infty < x < 0)$ y' is increasing.

The extreme values of y' are:

$$y'\,(-\infty) = -\,m$$

$$y'\,(0) = -\,m - (m\,\varepsilon_M^{(M)} + \varepsilon_o^{M}) - 2\rho_o^{M}$$

If $\varepsilon_o^{(M)} + m\,\varepsilon_M^{(M)} + 4\,\rho_o^{(M)} < 0$, and $\rho_o^{(M)} > 0$, this implies

1) $\varepsilon_o^{(M)} + m\,\varepsilon_M^{(M)} < 0$

2) $\varepsilon_o^{(M)} + m\,\varepsilon_M^{M} + 2\rho_o^{M} < 0$

a-1 $\quad - m - (\varepsilon_o^{(M)} + m\,\varepsilon_M^{(M)} + 2\rho_o^{(M)}) < 0$

y' is always negative. y is always decreasing

a-2 $\quad - m - (\varepsilon_o^{(M)} + m\,\varepsilon_M^{(M)} + 2\rho_o^{(M)}) > 0$

y' is zero only once.

y is decreasing, passes through a minimum then increases.

Case b

$$\varepsilon_o^{(M)} + m\,\varepsilon_M^{(M)} + 4\rho_o^{(M)} > 0$$

Assuming $\varepsilon_o^{(M)} + m\,\varepsilon_M^{(M)} < 0$, y, passes through zero once. Then y" is positive, then negative; y' is increasing, and decreasing

<u>b-1</u> $- m - (\varepsilon_o^{(M)} + m\,\varepsilon_M^{(M)} + 2\rho_o^{(M)}) > 0$

y' is zero only once, negative first, and positive after.

Therefore y is decreasing, passes through a minimum and increases thereafter

<u>b-2</u> $- m - (\varepsilon_o^{(M)} + m\,\varepsilon_M^{(M)} + 2\rho_o^{(M)}) < 0$

<u>b-2-a</u> y' is always negative, and y is always decreasing

<u>b-2-b</u> y' is negative, zero, passes through a maximum and is zero and negative again. y passes through a minimum and a maximum.

This discussion is summarized in the following table.

	function	$u < 0$	$u > 0$
$v < 0$	y_1	< 0	< 0
	y''	> 0	> 0
	y'	$-m$ ↗ u	$-m$ ↗ ↗ u
	y	↘	↘ ↗
$v > 0$	y_1	↗ 0 ↗	↗ 0 ↗
	y''	>0 <0	>0 <0
	y'	$-m$ ↗ ↘	$-m$ ↗ 0 ↗ ↘ >0
	y	↘ ↗ ↘ ↘	↘ ↗

$$u = -m - \varepsilon_o^{(M)} + m\,\varepsilon_M^{(M)} + 2\rho_o^{(M)}$$

$$v = \varepsilon_o^{(M)} + m\,\varepsilon_M^{(M)} + 4\rho_o^{(M)}$$

In order to compare the effects of first and second order interaction with the effect of first order above, the later was also investigated. The equations are:

$$y = \ln K - m\,x - (\varepsilon_o^{(M)} + m\,\varepsilon_M^{(M)})\,e^x \qquad (8)$$

$$y' = -m - (\varepsilon_o^{(M)} + m\,\varepsilon_M^{(M)})\,e^x$$

$$y'' = -(\varepsilon_o^{(M)} + m\,\varepsilon_M^{(M)})$$

<u>Case 1</u> $\varepsilon_o^{(M)} + m\,\varepsilon_M^{(M)} < 0$

y" is positive. y' is increasing on the interval $(-\infty, 0)$

The extreme values are:

$$y'(-\infty) = -m$$

$$y'(0) = -m - (\varepsilon_o^{(M)} + m\,\varepsilon_M^{(M)})$$

<u>1-1</u> $-m - (\varepsilon_o^{(M)} + m\,\varepsilon_M^{(M)}) > 0$

y' passes through zero once. y decreases, passes through a minimum and increases.

<u>1-2</u> $-m - (\varepsilon_o^{(M)} + m\,\varepsilon_M^{(M)}) < 0$

y' is always negative. y always decreases.

<u>Case 2</u>

$\varepsilon_o^{(M)} + m\varepsilon_M^{(M)} > 0$

y" is negative. y' is decreasing and negative.

y is always decreasing

This can be summarized in the following table.

	$\varepsilon_o^{(M)}+m\varepsilon_M^M > 0$	
y''	< 0	
y'	< 0	
y	↘	
	$\varepsilon_o^{(M)}+m\,\varepsilon_M^M < 0$	
	$-m-(\varepsilon_o^{(M)}+m\,\varepsilon_M^{(M)})>0$	$-m-(\varepsilon_o^{(M)}+m\,\varepsilon_M^{(M)})<0$
y''	> 0	> 0
y'	$-m$ ↗ 0 ↗	< 0
y	↘ ↗	↘

The main difference is that y cannot have a maximum.

The results have been presented and discussed in the case of chromium in the text.

REFERENCES

1. C. Wagner, Thermodynamics of Alloys, p.51, Addison-Wesley, Reading, Massachusetts (1962).
2. J. Chipman, J. Iron Steel Inst. 180, 97 (1955).
3. C. H. P. Lupis and J. F. Elliott, Trans. Met. Soc. of AIME, 233, 257, (1965).
4. C. H. P. Lupis and J. F. Elliott, Trans. Met. Soc. of AIME, 233, 829, (1965).
5. C. H. P. Lupis and J. F. Elliott, Acta. Met. 14, 529 (1966).
6. H. M. Chen and J. Chipman, Trans. ASM (1947), 38, 70 - 113.
7. E. T. Turkdogan, J.I.S.I. (1954), 178, 278.
8. A. McLean and H. B. Bell, J.I.S.I., (1965) 203, p.123 - 130.
9. J. Chipman, J.I.S.I. (1955), 180, 97 - 106.
10. H. Sakao and K. Sano, J. Japan Inst. Met., vol. 4, 236-244.
11. S. Matoba and T. Kuwana, Tetsu-to-Hagane, (1965), 5, No. 3, 187-195.
12. N. A. Gokcen, Trans. AIME, (1956), 206, 1558.
13. E. S. Tankins, N. A. Gokcen and G. R. Belton, Trans. AIME, (1964), 203, 820.
14. J. Chipman, Trans. I.S.I.J. (1966), 6, 207-216.
15. L. S. Darken and R. W. Gurry, Physical Chemistry of Metals, McGraw-Hill Books Co., (1953).
16. J. Chipman, J. Am. Chem. Soc. (1933), 55, 3131.
17. J. G. Thompson, H. C. Vacher and H. A. Bright, Trans. AIME, (1937), 125, 246.
18. M. G. Fontana and J. Chipman, Trans. ASM (1936), 24, 313.
19. J. Chipman and A. M. Samarin, Trans. AIME (1937), 125, 331.
20. M. N. Dastur and J. Chipman, Trans. AIME (1949), 185, 445.
21. T. P. Floridis and J. Chipman, Trans. Met. Soc. AIME, (1958), 212, 549.
22. V. V. Averin, A. Y. Polyakov, and A. M. Samarin, Izv. Akad. Nauk. SSSR., Otd. Tekhu. Nauk. (1955), 3, 90.

23. S. Matoba and Y. Gunji, Nikou Gakujutsu Shinkokai, 19th Committee Report, April (1959), No. 5425.

24. P. H. Emmet and J. F. Schultz, J. Am. Chem. Soc. (1933), 55, 1376.

25. L. S. Darken and R. W. Gurry, J. Am. Chem. Soc., (1945), 67, 1398.

26. M. N. Dastur and J. Chipman, Disc. Faraday Soc., (1948), 4, 100.

27. H. Sakao and K. Sano, Trans. Japan Inst. Metals, (1960), 1, 38.

28. J. Bockris , J. White and J. Mackenzie, Physicochemical Measurements at High Temperatures, Butterworths Scientific Publications, (1959).

29. J. C. d'Entremont, Trans. Met. Soc. AIME (1963), 227, 482.

30. P. Kosakevitch and G. Urbain, Mem. Sci. Rev. Met., (1961), 58, 401.

31. S. Y. Shiraishi, M.Sc. Thesis, McMaster University, (1966).

32. J. K. Pargeter, Can. Met. Quart., (1967) 6, No. 1, 21.

33. L. Enskog, Physik Z., (1911), 12, 56 and 533.

34. S. Chapman, Phil. Trans. Roy. Soc. A., (1916), 216, 279.

35. S. Chapman, ibid, (1917), 217, 110.

36. S. Chapman and F. Dootson, Phil. Mag., (1917), 33, 248.

37. L. S. Darken and R. W. Gurry, J. Am. Chem. Soc. (1945), 67, 1398.

38. L. J. Gillepsie, J. Chem. Phys., (1939) 7, 530.

39. G. W. Toop and F. D. Richardson, Advances in Extractive Metallurgy, The Institution of Mining and Metallurgy, London (1967).

40. P. Kershaw, Private communication.

41. G. P. Baxter and J. E. Lansing, J. Amer. Chem. Soc., (1920), 42, 419.

42. J. B. Bookey, J.I.S.I., (1952), 172, 66 and ibid., 86.

43. H.F. Ramstad and J. Richardson, Trans. A.I.M.E. (1961) 221, p.1021.

44. A. Smellie, Ph.D. thesis (1968), University of Strathclyde, Glasgow.

45. D. Gommersal, Ph.D. Thesis (1967), McMaster University, Hamilton.

46. R. Baker, J.I.S.I., (1967), 205, p.637.

47. M. R. Spiegel, Theory and problems of statistics, Schaum pub. New York, (1961).

48. J. Elliott and M. Gleiser, Thermochemistry for steelmaking, vol. 1, Addison Wesley (1960).

49. Ibid, p.176.

50. S. Marshall and J. Chipman, Trans. ASM, (1942), 30, No. 3, 695.

51. J. Elliott, M. Gleiser and V. Ramakrishna, Thermochemistry for Steelmaking, Vol. II, Addison Wesley (1963).

52. A. Rist and J. Chipman, Revue de Metallurgie, (1956), 53, No. 10, 796.

53. J. Belton, University of Pennsylvania, Private communication.

54. D. C. Hilty, W. D. Forgeng and R. L. Folkman, Trans. AIME, (1955), p.253.

55. J. d'Entremont, D. Guernsey and J. Chipman, Trans. AIME, (1963), 227, No. 1, p.14.

56. J. Chipman and D. Corrigan, Trans. AIME (1965), vol. 233, p.1249.

57. C. H. P. Lupis and J. F. Elliott, Acta. Met., (1967), vol. 15, 265.

58. T. L. Hill, Introduction to Statistical Thermodynamics, (1960) Addison-Wesley Publishing Co., Reading, Mass.

59. Handbook of Chemistry and Physics (1968). The Chemical Rubber Co.

60. Janaf,Thermochemical data, Thermal Research Laboratory, The Dow Chemical Co. (1961).

61. K. Charlton, Ph.D. Thesis, (1963), University of Glasgow.

62. H. C. Vacher, Journal of Research, U.S. Bureau of Standards (1933) vol. 11, p.541.

TABLE I

Definitions of interaction coefficients

(at $X_1 \rightarrow 1$, or % 1 → 100)

Order	Free Energy		Entropy		Enthalpy		System for
	X	%	X	%	X	%	obtaining property
zero	$\ln\gamma_i^o$	$\log f_i = 0$	$S_i^{E^o}$	$\mathcal{S}_i^{E^o} = 0$	$H_i^{E^o}=0$	$\mathcal{H}_i^{E^o}=0$	1-i binary
first	$\varepsilon_i^{(i)}$	$e_i^{(i)}$	$\sigma_i^{(i)}$	$s_i^{(i)}$	$\eta_i^{(i)}$	$h_i^{(i)}$	1-i binary
second	$\rho_i^{(i)}$	$r_i^{(i)}$	$\pi_i^{(i)}$	$p_i^{(i)}$	$\lambda_i^{(i)}$	$l_i^{(i)}$	1-i binary
	$\rho_i^{(j)}$	$r_i^{(j)}$	$\pi_i^{(j)}$	$p_i^{(j)}$	$\lambda_i^{(j)}$	$l_i^{(j)}$	1-i-j ternary
	$\rho_i^{(j,k)}$	$r_i^{(j,k)}$	$\pi_i^{(j,k)}$	$p_i^{(j,k)}$	$\lambda_i^{(j,k)}$	$l_i^{(j,k)}$	1-i-j-k quaternary

Representative Equations:

$$\ln \gamma_i = \ln\gamma_1{}^o + \sum_{j=2}^{m} \varepsilon_i^{(j)} X_j + \sum_{j=2}^{m} \sum_{k=2}^{m} \rho_i^{(j,k)} X_j X_k + \theta (X^3)$$

$$\log f_i = \sum_{j=2}^{m} e_i^{(j)} (\% j) + \sum_{j=2}^{m} \sum_{k=2}^{m} r_i^{(j,k)} (\% j) (\% k) + 0 (\%^3)$$

TABLE II

Chromium-oxygen interaction parameters at 1600°C

Author	Ref.	$\varepsilon_O^{(Cr)}$*	$e_O^{(Cr)}$	Range of Cr investigation wt. pct.
Chen and Chipman **	6, 9	- 8.7	-0.041	0 - 10
Turkdogan	7	-13.7	-0.064	0 - 12
McLean and Bell	8	-12.4	-0.058	0 - 10
Sakao and Sano	10	- 9.58	-0.045	
Matoba and Kuwana	11	- 7.87	-0.037	<12
Pargeter	32	-11.1	-0.052	0 - 8
Charlton	61	-12.7	-0.059	0 - 10

* Computed value from e_O^{Cr} , with formula (1.2)

** Temperature = 1595°C

TABLE III

Analyses of materials used.

I Iron

Elements	C	Mn	S	P	Si	Cu	Ni	Cr	Al	N
Armco	.024	.033	.015	.005	.001	.018				
Ferrovac E	.005	.001	.006	.002	.006	ND	ND	ND	ND	.004

II Chromium: 99.95 wt. pct. Cr

(provided by McKay Inc.)

III Aluminum 99.9995 wt. pct. Al

TABLE IV

SYSTEM FE-O
TEMPERATURE 1600 C
KINETIC RUNS

RUN NO	ATM. PRES. MM HG	PRES. DROP MM HG	WATER BATH T OC	PH2O/PH2 X 10^2	O CONTENT P.P.M.	LOG K_1	TIME MIN.
1101	756.2	1.5	33.6	5.452	130	0.623	1
1102	756.1	1.5	33.6	5.452	135	0.606	1
1103	755.7	1.5	33.6	5.456	184	0.472	1
1104	754.7	1.5	33.6	5.463	159	0.536	1
1105	754.7	1.5	33.6	5.463	155	0.547	1
1106	751.2	1.5	33.6	5.490	171	0.507	1
1107	751.9	1.5	33.6	5.485	136	0.606	3
1108	751.9	1.5	33.6	5.485	140	0.593	3
1110	751.4	1.5	33.6	5.489	158	0.541	3
1111	758.6	1.5	33.6	5.434	109	0.698	5
1112	758.2	1.5	33.6	5.437	111	0.690	5
1113	758.2	1.5	33.6	5.437	123	0.645	5
1114	757.4	1.5	33.6	5.443	121	0.653	5
1115	756.9	1.5	33.6	5.446	149	0.563	5
1116	756.8	1.5	33.6	5.447	128	0.629	5
1117	756.8	1.5	33.6	5.447	134	0.609	5
1118	750.3	1.5	33.6	5.497	119	0.665	5
1121	754.0	1.5	33.6	5.469	132	0.617	5
1122	754.0	1.5	33.6	5.469	103	0.725	5
1123	753.5	1.5	33.6	5.472	102	0.730	5
1124	753.8	1.5	33.6	5.470	117	0.670	5
1125	753.7	1.5	33.6	5.471	96	0.756	5
1128	752.6	1.5	33.6	5.472	101	0.734	5

Samples 1116 to 1125 deoxidized 2 minutes in hydrogen - all other not deoxidized.

TABLE V

SYSTEM FE-O

TEMPERATURE 1550 C

RUN NO	ATM. PRESSURE MM HG	PRESSURE DROP MM HG	WATER BATH T OC	PH2O/PH2 X 10^2	O CONTENT P.P.M.	LOG K_1
1438	756.0	0.4	32.7	5.160	75	0.838
1440	755.7	0.4	32.7	5.162	86	0.778
1441	755.4	0.4	32.7	5.164	73	0.850
1442	755.4	0.4	32.7	5.164	87	0.773
1443	755.4	0.4	32.7	5.164	65	0.820
1444	751.2	0.4	32.7	5.194	75	0.840
1445	751.0	0.4	32.7	5.196	75	0.842
1447	750.3	0.4	32.7	5.201	77	0.830

Samples exposed to H_2-H_2O atmosphere, at 1550°C, for at least 10 minutes.

TABLE VI

SYSTEM FE-O

TEMPERATURE 1600 C

RUN NO	ATM. PRESSURE MM HG	PRESSURE DROP MM HG	WATER BATH T OC	P_{H_2O}/P_{H_2} X 10^2	O CONTENT P.P.M.	LOG K_1
1023	756.4	1.5	34.6	5.782	106	0.737
1024	756.4	1.5	34.6	5.782	104	0.745
1025	756.4	1.5	34.6	5.782	132	0.642
1026	756.8	1.5	34.6	5.779	101	0.758
1027	756.7	1.5	34.6	5.780	122	0.676
1028	756.7	1.5	34.6	5.780	104	0.745
1029	756.6	1.5	34.6	5.781	113	0.709
1030	756.6	1.5	34.6	5.781	98	0.771

TABLE VII

SYSTEM FE-O

TEMPERATURE 1600 C

EFFECT OF WEIGHT OF SAMPLE AND FLOWRATE OF GAS

runs 1140 to 1156 weight = 1.4g. flow rate = 4300 cc/min.

runs 1158 to 1163 weight = 0.6g. flow rate = 400 cc/min.

RUN NO	ATM. PRESSURE MM HG	PRESSURE DROP MM HG	WATER BATH T OC	P_{H2O}/P_{H2} X 10^2	O CONTENT P.P.M.	LOG K_1
1140	766.3	2.1	33.7	56.57	1024	0.742
1141	766.7	2.2	33.7	56.56	1051	0.731
1142	766.6	2.1	33.7	56.56	965	0.768
1143	766.5	2.1	33.7	56.56	1019	0.744
1144	766.3	2.1	33.7	56.56	971	0.765
1151	748.7	2.0	33.8	57.52	1170	0.691
1152	748.7	2.0	33.8	57.52	1060	0.735
1153	748.7	2.0	33.8	57.52	1175	0.690
1154	749.3	2.0	33.8	57.47	1100	0.718
1155	749.3	2.0	33.8	57.47	1057	0.735
1156	749.3	2.0	33.8	57.47	1007	0.756
1158	761.7	1.2	33.7	56.08	1185	0.675
1159	761.6	1.2	33.7	56.09	974	0.760
1160	761.4	1.2	33.7	56.10	1026	0.739
1161	761.5	1.2	33.7	56.09	1116	0.701
1162	761.5	1.2	33.7	56.09	937	0.777
1163	761.5	1.2	33.7	56.09	990	0.753

TABLE VIII

SYSTEM FE-O

TEMPERATURE 1650 C

RUN NO	ATM. PRESSURE MM HG	PRESSURE DROP MM HG	WATER BATH T OC	PH2O/PH2 X 10^2	O CONTENT P.P.M.	LOG K_1
1301	745.4	0.5	33.8	5.594	139	0.605
1302	746.0	0.5	33.8	5.589	163	0.535
1303	746.0	0.6	33.8	5.590	142	0.595
1304	745.9	0.5	33.8	5.590	149	0.574
1305	745.9	0.5	33.8	5.590	151	0.568
1306	746.0	0.6	33.8	5.590	153	0.563
1307	745.4	0.5	33.8	5.594	137	0.611
1308	745.4	0.5	33.8	5.594	132	0.627
1309	745.4	0.5	33.8	5.594	130	0.634
1310	745.4	0.5	33.8	5.594	140	0.602

TABLE IX

SYSTEM FE-O

TEMPERATURE 1700 C

RUN NO	ATM. PRESSURE MM HG	PRESSURE DROP MM HG	WATER BATH T OC	$P_{H2O}/P_{H2} \times 10^2$	O CONTENT P.P.M.	LOG K_1
1312	743.8	0.5	33.8	5.606	182	0.489
1313	743.8	0.5	33.8	5.606	181	0.491
1314	743.8	0.5	33.8	5.606	183	0.486
1315	744.7	0.5	33.8	5.599	183	0.486
1316	744.7	0.5	33.8	5.599	201	0.445
1317	746.7	0.5	33.8	5.583	170	0.516
1318	746.7	0.5	33.8	5.583	176	0.501
1319	747.1	0.5	33.8	5.580	198	0.450
1320	747.1	0.5	33.8	5.580	186	0.477

TABLE X

SYSTEM FE-O

TEMPERATURE 1750 C

RUN NO	ATM. PRESSURE MM HG	PRESSURE DROP MM HG	WATER BATH T OC	PH2O/PH2 X 10^2	O CONTENT P.P.M.	LOG K_1
1420	758.2	0.4	32.7	5.144	213	0.383
1421	758.2	0.4	32.7	5.144	218	0.373
1422	764.5	0.4	32.7	5.099	192	0.424
1423	764.4	0.4	32.7	5.100	210	0.385
1424	764.4	0.4	32.7	5.100	201	0.404
1426	763.9	0.4	32.7	5.104	221	0.364
1427	763.4	0.4	32.7	5.107	187	0.436

TABLE XI

SYSTEM FE-O

EFFECT OF TEMPERATURE ON LOG K_2

RUN NO	PCO2/PCO X 10^2	O CONTENT P.P.M.	LOG K_2	TEMP. 0 C
1241	5.641	483	0.067	1550
1242	5.641	475	0.075	1550
1243	5.641	477	0.073	1550
1244	5.641	471	0.078	1550
1245	5.641	476	0.074	1550
1213	5.641	560	0.003	1600
1214	5.641	577	-0.010	1600
1215	5.641	542	0.017	1600
1216	5.641	579	-0.011	1600
1217	5.641	603	-0.029	1600
1218	5.641	614	-0.037	1600
1219	5.641	539	0.020	1600
1220	5.641	549	0.012	1600
1221	5.641	698	-0.092	1650
1222	5.641	778	-0.140	1650
1223	5.641	730	-0.112	1650
1224	5.641	699	-0.093	1650
1225	5.641	702	-0.095	1650
1226	5.641	759	-0.129	1650
1229	5.641	883	-0.195	1700
1230	5.641	935	-0.219	1700
1231	5.641	887	-0.196	1700
1232	5.641	941	-0.222	1700
1233	5.641	981	-0.220	1700
1265	5.641	1066	-0.276	1750
1266	5.641	1048	-0.269	1750
1267	5.641	1223	-0.336	1750
1268	5.641	1333	-0.373	1750
1269	5.641	1301	-0.363	1750
1270	5.641	1406	-0.397	1750

TABLE XII

SYSTEM FE-O

EFFECT OF OXYGEN CONTENT ON LOG K_2

RUN NO	PCO2/PCO X 10^2	O CONTENT P.P.M.	LOG K_2	TEMP. O C
1246	2.030	201	0.004	1600
1247	2.030	228	-0.050	1600
1248	2.030	214	-0.023	1600
1249	2.030	227	-0.048	1600
1250	2.030	216	-0.027	1600
1251	2.030	214	-0.023	1600
1212	5.474	643	-0.069	1600
1213	5.641	560	0.003	1600
1214	5.641	577	-0.010	1600
1215	5.641	542	0.017	1600
1216	5.641	579	-0.011	1600
1217	5.641	603	-0.029	1600
1218	5.641	614	-0.037	1600
1219	5.641	539	0.020	1600
1220	5.641	549	0.012	1600
1252	9.111	821	0.045	1600
1253	9.111	841	0.035	1600
1255	9.111	836	0.037	1600
1256	9.111	829	0.041	1600
1257	9.111	832	0.039	1600
1277	9.111	936	-0.012	1600
1278	9.111	1086	-0.076	1600
1279	9.111	1006	-0.043	1600
1280	9.111	1016	-0.047	1600
1366	14.025	1587	-0.054	1600
1367	14.025	1459	-0.017	1600
1368	14.025	1497	-0.029	1600
1371	14.025	1504	-0.030	1600
1372	14.025	1518	-0.034	1600
1373	14.025	1556	-0.045	1600
1259	17.647	1791	-0.006	1600
1260	17.647	1839	-0.018	1600
1261	17.647	1744	0.005	1600
1262	17.647	1790	-0.006	1600
1263	17.647	1666	0.025	1600
1281	17.647	1631	0.034	1600
1284	17.647	1902	-0.032	1600
1285	17.647	1819	-0.013	1600
1286	17.647	1652	0.029	1600

TABLE XIII

SYSTEM FE-C

TEMPERATURE 1550 C

OXYGEN POTENTIAL CONTROLLED BY CO/CO2

KINETIC RUNS

RUN NO	PCO2/PCO X 10^2	C CONTENT P.P.M.	LOG K_2	TIME MIN.
1289	5.641	18	1.496	0
1290	5.641	433	0.115	2
1299*	5.641	643	-0.057	5
1360	5.641	416	0.132	10
1241	5.641	483	0.067	15
1242	5.641	475	0.075	15
1243	5.641	477	0.073	15
1244	5.641	471	0.078	15
1245	5.641	476	0.074	15
1288	5.641	450	0.098	15
1361*	5.641	472	0.077	15
1362	5.641	504	0.049	30
1363	5.641	504	0.049	30
1364	5.641	465	0.084	30

*Samples not deoxidized - All other deoxidized 4 minutes in hydrogen.

TABLE XIV

Comparison of data for log K_2

Authors	log K_2	Temperature range-°C
Gokcen(12)	8088/T - 4.438	1550 - 1700
Gokcen Serie D(12)	8088/T - 4.468	
Vacher(62)	0.003	1580°C
Marshall and Chipman(50)	7320/T - 3.960	1550 - 1700
Present work	8421/T - 4.519	1550 - 1750

TABLE XV

Comparison of data for log K_1

Authors	log K_1	Temperature range-^oC
Averin et al(22)	9440/T - 4.536	1550 - 1700
Tankins et al(13)	6817/T - 3.13	1550 - 1700
Sakao and Sano(10)	7040/T - 3.224	1550 - 1650
Matoba and Kuwana(11)	7480/T - 3.42	1550 - 1663
Dastur and Chipman(20)	7050/T - 3.17	1755 - 1760
Floridis and Chipman(21)	7050/T - 3.20	1550 - 1600
Present work	7054/T - 3.16	1550 - 1750

TABLE XVI

TEMPERATURE 1600 C

SYSTEM FE-O-CR

OXYGEN POTENTIAL CONTROLLED BY CO/CO2

RUN NO	PCO2/PCO X 10^2	O CONTENT P.P.M.	LOG K_2	CR CONTENT W/O
1273	2.030	238	-0.069	1.00
1274	2.030	249	-0.089	1.00
1275	2.030	247	-0.085	1.00
1276	2.030	300	-0.170	1.00
1380	1.781	297	-0.222	1.95
1381	1.781	260	-0.164	1.95
1382	1.781	295	-0.219	1.95
1384	1.781	294	-0.218	2.02
1385	1.781	301	-0.228	2.02
1375	0.523	118	-0.354	3.92
1373	0.523	129	-0.392	3.92
1377	0.523	110	-0.323	3.92
1378	0.523	200	-0.533	9.99
1376	0.523	180	-0.537	9.99

TABLE XVII

SYSTEM FE-O-CR

TEMPERATURE 1550 C

RUN NO	ATM. PRESS. MM HG	PRESS. DROP MM HG	WATER BATH T OC	PH2O/PH2 X 10^2	O CONTENT P.P.M.	LOG K_1	CR CONTENT W/O
1386	749.3	0.3	32.7	5.207	91	0.758	1.00
1387	749.3	0.3	32.7	5.207	97	0.730	1.00
1388	747.9	0.3	32.7	5.218	81	0.809	1.00
1389	747.2	0.3	32.7	5.223	98	0.727	2.02
1390	745.8	0.3	32.7	5.235	107	0.690	2.02
1391	744.9	0.3	32.7	5.240	112	0.670	2.02
1392	744.1	0.3	32.7	5.246	128	0.613	3.92
1393	743.7	0.3	32.7	5.249	128	0.613	3.92
1394	743.4	0.3	32.7	5.251	132	0.600	3.92
1450	744.9	0.1	48.9	2.002	99	0.306	7.67
1451	745.8	0.1	48.9	2.000	94	0.328	7.67
1452	743.5	0.1	48.9	2.006	83	0.383	7.67
1453	743.5	0.0	48.9	2.006	103	0.289	9.99
1455	743.1	0.0	48.9	2.007	115	0.242	9.99
1458	749.8	0.0	48.9	1.989	188	0.024	15.00
1460	750.1	0.0	48.9	1.988	135	0.168	15.00
1523	754.1	0.0	36.8	0.844	143	-0.229	24.00
1521	754.3	0.0	36.8	0.844	133	-0.198	24.00
1522	754.3	0.0	36.8	0.844	138	-0.214	24.00

Samples exposed to H_2-H_2O atmosphere, at 1550°C, for 30 minutes.

TABLE XVIII

SYSTEM FE-O-CR

TEMPERATURE 1600 C

RUN NO	ATM. PRESS. MM HG	PRESS. DROP MM HG	WATER BATH T OC	PH2O/PH2 X 10^2	O CONTENT P.P.M.	LOG K_1	CR CONTENT W/O
1331	752.3	0.5	33.8	5.539	121	0.661	0.52
1333	753.6	0.5	33.8	5.529	118	0.671	0.52
1334	753.6	0.5	33.8	5.529	116	0.678	0.52
1335	753.6	0.5	33.8	5.529	127	0.639	0.52
1321	747.1	0.5	33.8	5.580	99	0.751	1.01
1322	746.6	0.5	33.8	5.584	110	0.706	1.01
1323	746.6	0.5	33.8	5.584	113	0.694	1.01
1324	741.7	0.5	33.8	5.623	114	0.693	1.01
1325	741.7	0.5	33.8	5.623	113	0.697	1.01
1350	760.3	0.5	33.8	5.478	160	0.535	1.95
1351	760.3	0.5	33.8	5.478	165	0.521	1.95
1353	759.7	0.5	33.8	5.482	161	0.532	1.95
1461	750.0	0.0	48.9	1.988	92	0.335	7.67
1462	750.0	0.0	48.9	1.988	67	0.472	7.67
1463	750.0	0.0	48.9	1.988	80	0.395	7.67
1464	750.5	0.0	48.9	1.987	102	0.290	9.99
1465	750.4	0.0	48.9	1.987	125	0.201	9.99
1466	750.8	0.0	48.9	1.986	116	0.234	9.99
1467	751.2	0.0	48.9	1.985	195	0.008	15.00
1468	752.6	0.0	48.9	1.981	179	0.044	15.00
1469	751.6	0.0	48.9	1.984	186	0.028	15.00
1470	751.1	0.0	48.9	1.985	281	-0.151	19.99
1471	751.0	0.0	48.9	1.985	280	-0.149	19.99
1472	750.3	0.0	48.9	1.987	282	-0.152	19.99
1520	754.1	0.0	36.8	0.844	156	-0.267	24.00
1518	754.2	0.0	36.8	0.844	156	-0.267	24.00
1519	754.1	0.0	36.8	0.844	157	-0.270	24.00

Samples exposed to H_2-H_2O atmosphere, at 1600°C, for 15 minutes.

TABLE XIX

SYSTEM FE-O-CR

TEMPERATURE 1650 C

RUN NO	ATM. PRESS. MM HG	PRESS. DROP MM HG	WATER BATH T OC	PH2O/PH2 X 10^2	O CONTENT P.P.M.	LOG K_1	CR CONTENT W/O
1338	753.8	0.5	33.8	5.527	157	0.548	0.52
1339	753.8	0.5	33.8	5.527	165	0.526	0.52
1340	753.8	0.5	33.8	5.527	165	0.526	0.52
1326	745.5	0.5	33.8	5.593	160	0.544	1.01
1327	745.5	0.5	33.8	5.593	167	0.525	1.01
1328	745.5	0.5	33.8	5.593	171	0.516	1.01
1330	745.5	0.5	33.8	5.593	157	0.552	1.01
1430	759.8	0.5	32.7	5.133	155	0.520	2.02
1431	759.5	0.5	32.7	5.135	162	0.501	2.02
1432	759.2	0.5	32.7	5.137	166	0.491	2.02
1433	759.0	0.5	32.7	5.139	151	0.532	2.02
1434	758.5	0.4	32.7	5.142	202	0.406	3.92
1435	758.2	0.4	32.7	5.144	165	0.494	3.92
1437	756.9	0.4	32.7	5.153	188	0.438	3.92
1474	750.0	0.0	48.9	1.988	124	0.205	7.67
1475	750.0	0.0	48.9	1.988	106	0.273	7.67
1476	750.0	0.0	48.9	1.988	115	0.238	7.67
1477	749.9	0.0	48.9	1.988	139	0.155	9.99
1478	750.0	0.0	48.9	1.988	136	0.165	9.99
1479	749.8	0.0	48.9	1.989	134	0.172	9.99
1480	749.5	0.0	48.9	1.989	217	-0.038	15.00
1481	749.1	0.0	48.9	1.990	212	-0.027	15.00
1482	749.1	0.0	48.9	1.990	208	-0.019	15.00
1483	749.2	0.0	48.9	1.990	302	-0.181	19.99
1484	749.3	0.0	48.9	1.990	297	-0.174	19.99
1485	749.5	0.0	48.9	1.989	221	-0.046	19.99
1515	749.3	0.0	36.8	0.849	205	-0.383	24.00
1517	753.8	0.0	36.8	0.844	169	-0.302	24.00

Samples exposed to H_2 - H_2O atmosphere, at 1650°C, for 15 minutes.

TABLE XX

SYSTEM FE-O-CR

TEMPERATURE 1700 C

RUN NO	ATM. PRESS. MM HG	PRESS. DROP MM HG	WATER BATH T OC	PH2O/PH2 X 10^2	O CONTENT P.P.M.	LOG K_1	CR CONTENT W/O
1395	744.2	0.3	32.7	5.245	184	0.454	1.00
1397	744.6	0.3	32.7	5.242	178	0.469	1.00
1404	747.4	0.3	32.7	5.221	204	0.408	1.95
1403	748.6	0.3	32.7	5.213	205	0.405	1.95
1401	748.5	0.3	32.7	5.213	253	0.307	1.95
1398	745.0	0.3	32.7	5.239	236	0.346	1.95
1405	747.4	0.3	32.7	5.221	253	0.316	3.92
1406	747.4	0.3	32.7	5.221	234	0.348	3.92
1407	747.0	0.3	32.7	5.224	236	0.345	3.92
1486	754.1	0.0	48.9	1.977	116	0.232	7.67
1487	754.3	0.0	48.9	1.976	111	0.250	7.67
1488	754.2	0.0	48.9	1.977	122	0.210	7.67
1489	754.2	0.0	48.9	1.977	136	0.162	9.99
1490	754.4	0.0	48.9	1.976	150	0.119	9.99
1491	754.5	0.0	48.9	1.976	148	0.126	9.99
1492	754.4	0.0	48.9	1.976	240	-0.084	15.00
1493	754.4	0.0	48.9	1.976	229	-0.064	15.00
1494	754.5	0.0	48.9	1.977	230	-0.066	15.00
1496	754.0	0.0	48.9	1.977	331	-0.224	19.99
1497	755.2	0.0	48.9	1.974	357	-0.257	19.99
1509	747.8	0.0	36.8	0.851	183	-0.333	24.00
1510	748.0	0.0	36.8	0.851	184	-0.333	24.00
1511	748.4	0.0	36.8	0.850	184	-0.333	24.00

Samples exposed to H_2-H_2O atmosphere, at 1700°C, for 15 minutes.

TABLE XXI

SYSTEM FE-O-CR

TEMPERATURE 1750 C

RUN NO	ATM. PRESS. MM HG	PRESS. DROP MM HG	WATER BATH T OC	PH2O/PH2 X 10^2	O CONTENT P.P.M.	LOG K_1	CR CONTENT W/O
1416	758.3	0.3	32.7	5.142	228	0.353	0.51
1417	758.3	0.3	32.7	5.142	225	0.359	0.51
1418	758.3	0.3	32.7	5.142	242	0.327	0.51
1415	743.2	0.3	32.7	5.252	260	0.305	1.00
1408	746.1	0.3	32.7	5.231	275	0.279	1.95
1409	746.0	0.3	32.7	5.231	262	0.300	1.95
1412	743.2	0.3	32.7	5.252	315	0.222	3.92
1413	743.2	0.3	32.7	5.252	302	0.240	3.92
1414	743.2	0.3	32.7	5.252	351	0.175	3.92
1498	755.4	0.3	48.9	1.974	147	0.128	7.67
1499	755.4	0.3	48.9	1.974	142	0.143	7.67
1500	755.1	0.3	48.9	1.974	145	0.134	7.67
1507	755.1	0.0	48.9	1.974	169	0.067	9.99
1508	755.1	0.0	48.9	1.974	174	0.055	9.99
1502	755.1	0.3	48.9	1.974	269	-0.120	15.00
1503	755.1	0.3	48.9	1.974	269	-0.134	15.00
1505	755.2	0.3	48.9	1.974	269	-0.263	19.99
1506	755.2	0.3	48.9	1.974	357	-0.257	19.99
1497	754.0	0.3	48.9	1.977	357	-0.257	19.99
1512	748.5	0.0	36.8	0.850	192	-0.354	24.00
1513	748.7	0.0	36.8	0.850	200	-0.372	24.00

Samples exposed to H_2-H_2O atmosphere, at 1750°C, for 10 minutes.

TABLE XXII

Chromium-oxygen interaction parameters. Weight percent scale.

Temperature °C	$e_o^{(Cr)}$	$e_o^{(Cr)}$ calculated from (5.2)	$r_o^{(Cr)}$	$r_o^{(Cr)}$ calculated from (5.2)
1550	-0.068	- 0.067	10.6	9.5
1600	-0.059	- 0.059	6.8	7.6
1650	-0.051	- 0.051	6.0	5.8
1700	-0.037	- 0.043	1.6	4.1
1750	-0.041	- 0.037	4.6	2.5

$h_o^{(Cr)} = -2580$

$s_o^{(Cr)} = -1.107$

$\ell_o^{(Cr)} = 58.83$

$p_o^{(Cr)} = 2.79 \times 10^{-2}$

TABLE XXIII

Chromium-oxygen interaction parameters - mole fraction scale

Temperature °C	$\varepsilon_O^{(Cr)}$	$\varepsilon_O^{(Cr)}$ calculated from (5.2)	$\rho_O^{(Cr)}$	$\rho_O^{(Cr)}$ calculated from (5.2)
1550	-14.49	- 14.26	21.13	18.94
1600	-12.56	- 12.56	13.56	12.76
1650	-10.85	- 10.85	11.96	11.57
1700	- 7.85	- 9.14	3.19	8.18
1750	- 9.57	- 7.85	9.17	4.99

$\eta_O^{(Cr)} = -240100$

$\sigma_O^{(Cr)} = -103.2$

$\lambda_O^{(Cr)} = 104600$

$\pi_O^{(Cr)} = 556$

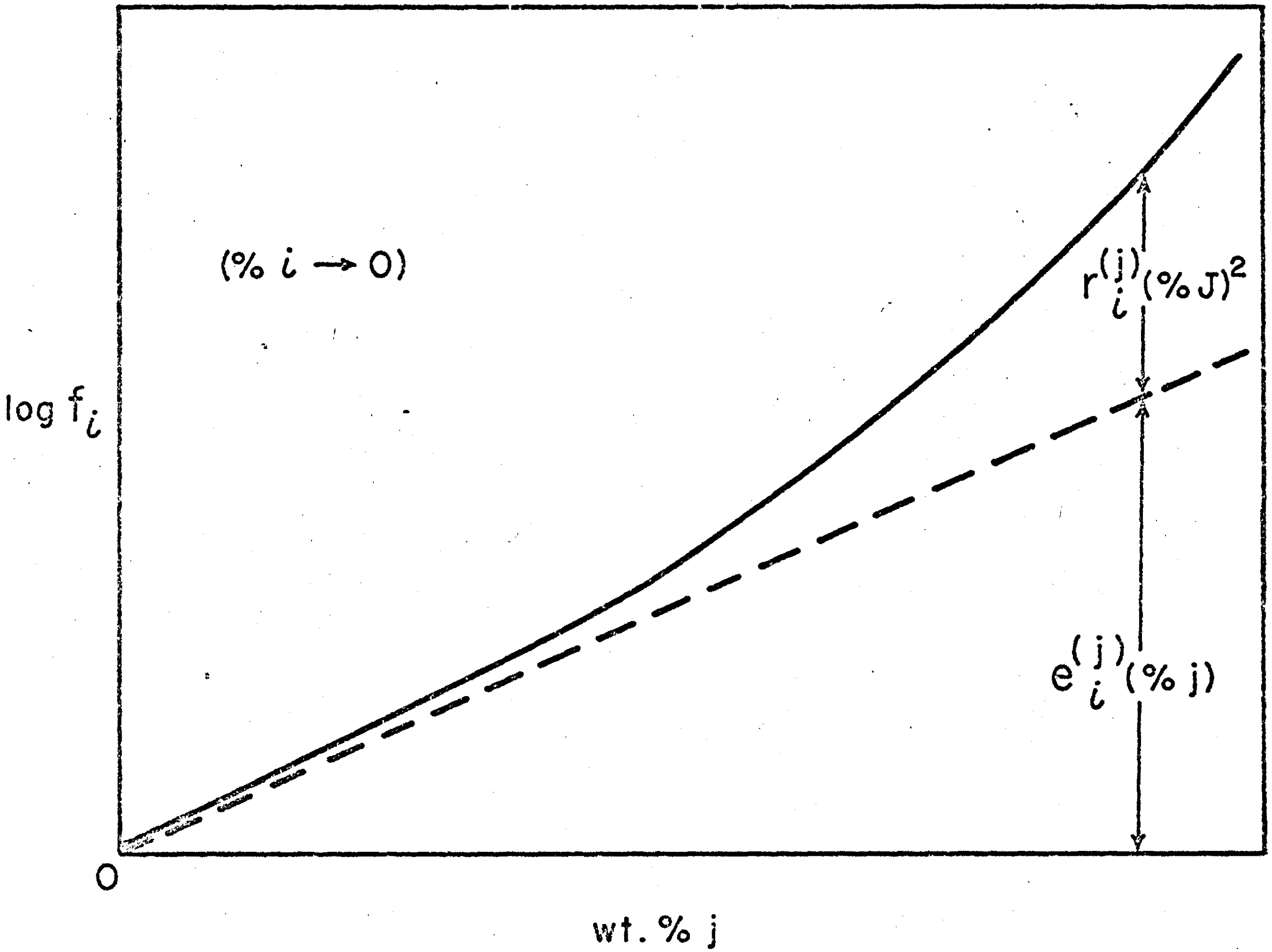

Figure 1. First and second order interaction coefficients in ternary 1-i-j systems.

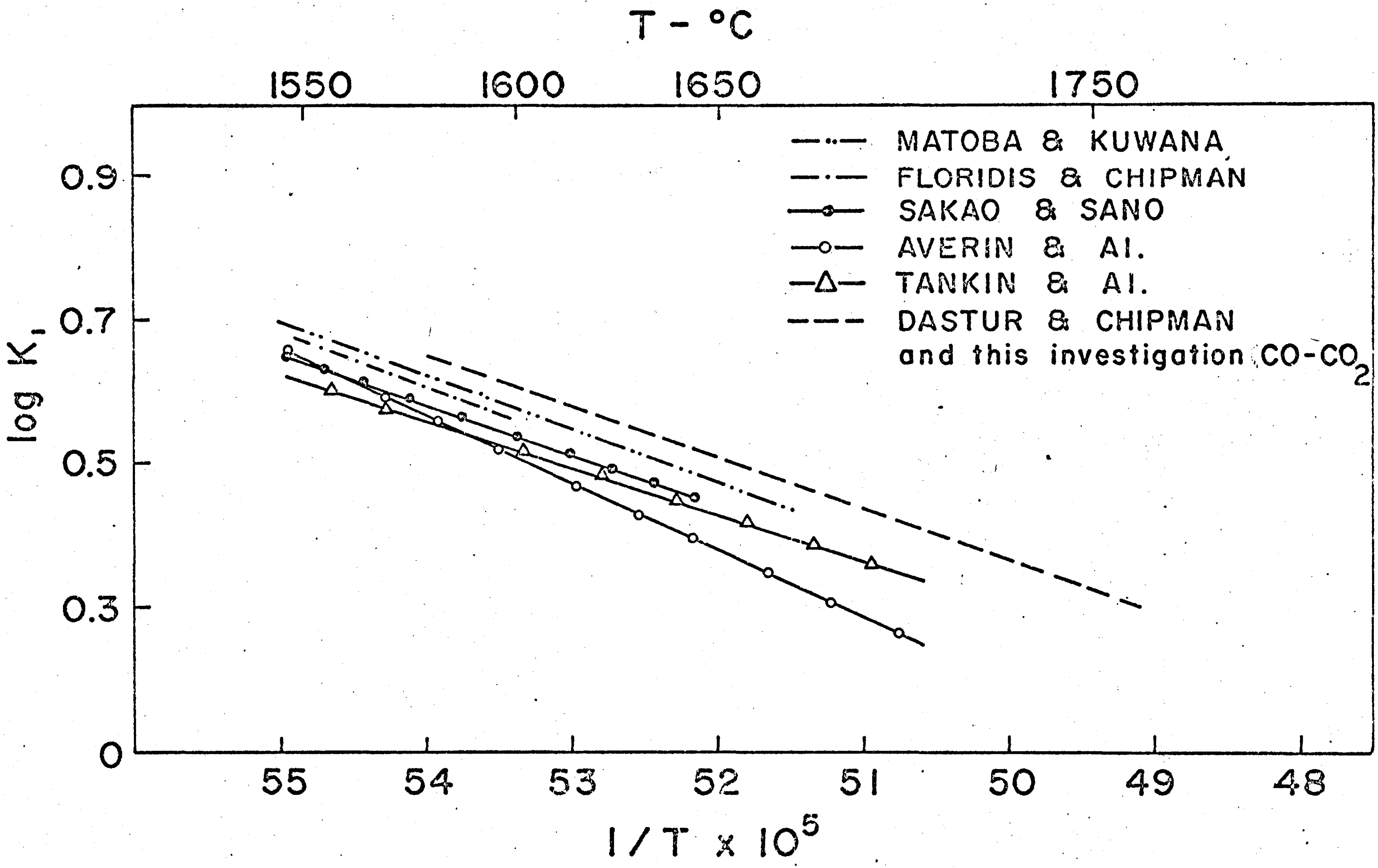

Figure 2. Variation of log k_1 with temperature. Results from various investigators.

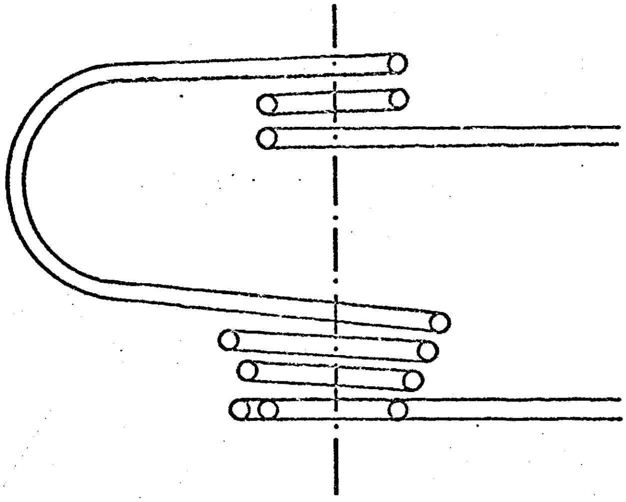

Coil No. 1

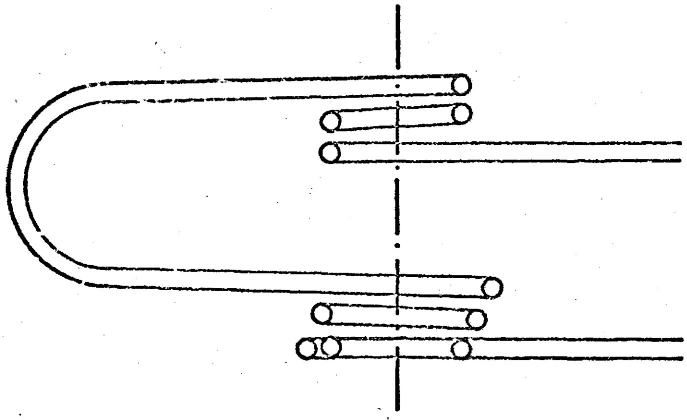

Coil No. 2

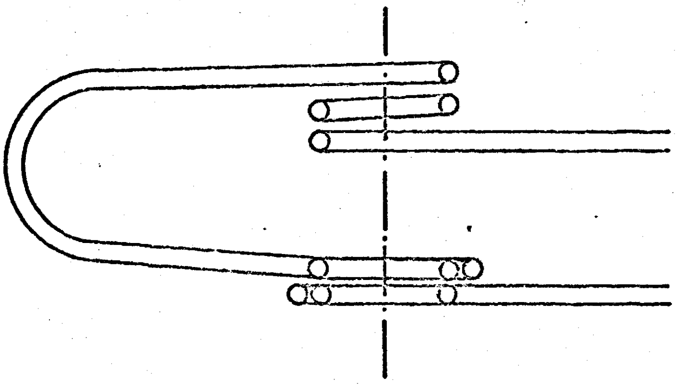

Coil No. 3

Figure 3. Coils designs.

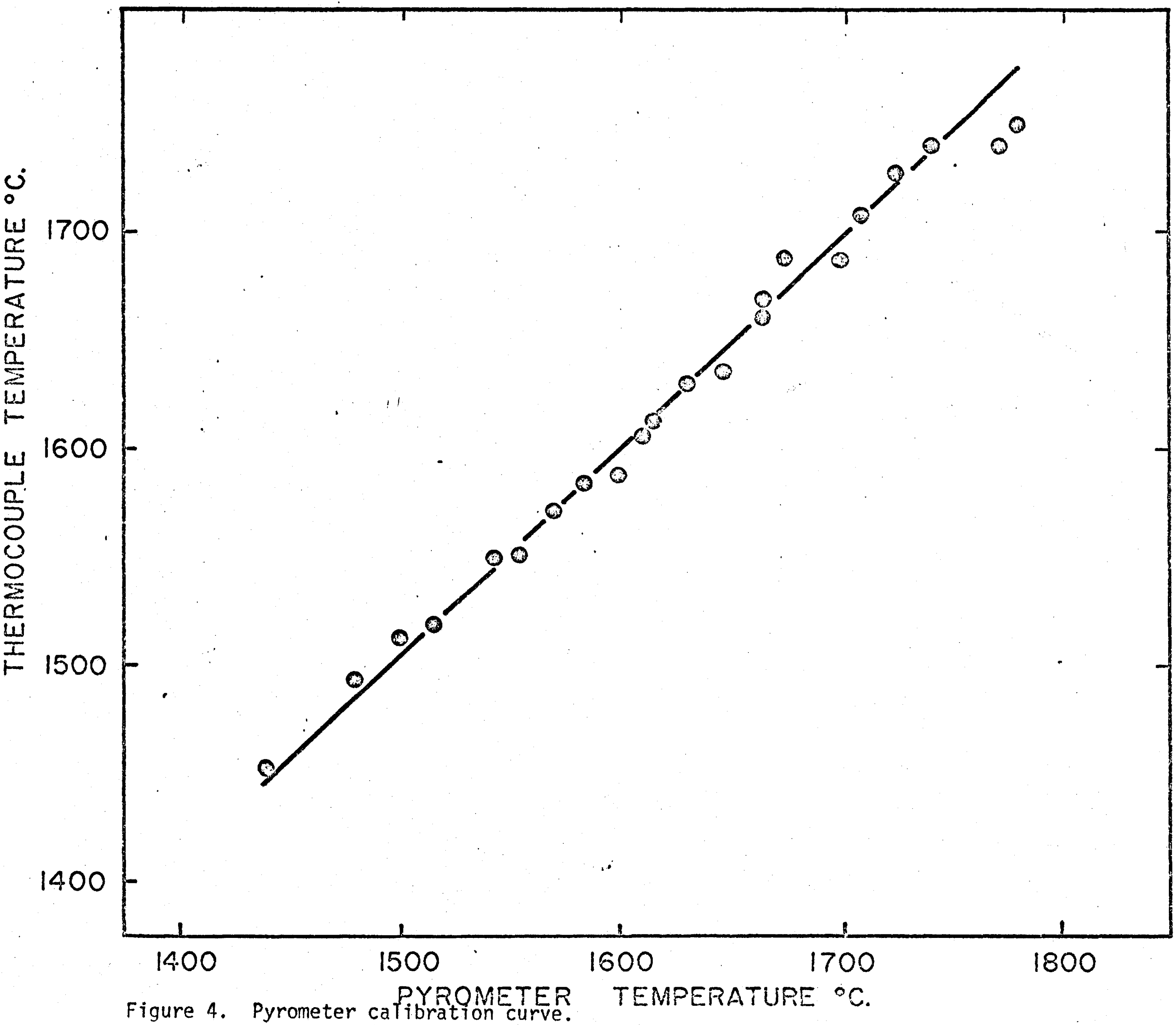

Figure 4. Pyrometer calibration curve.

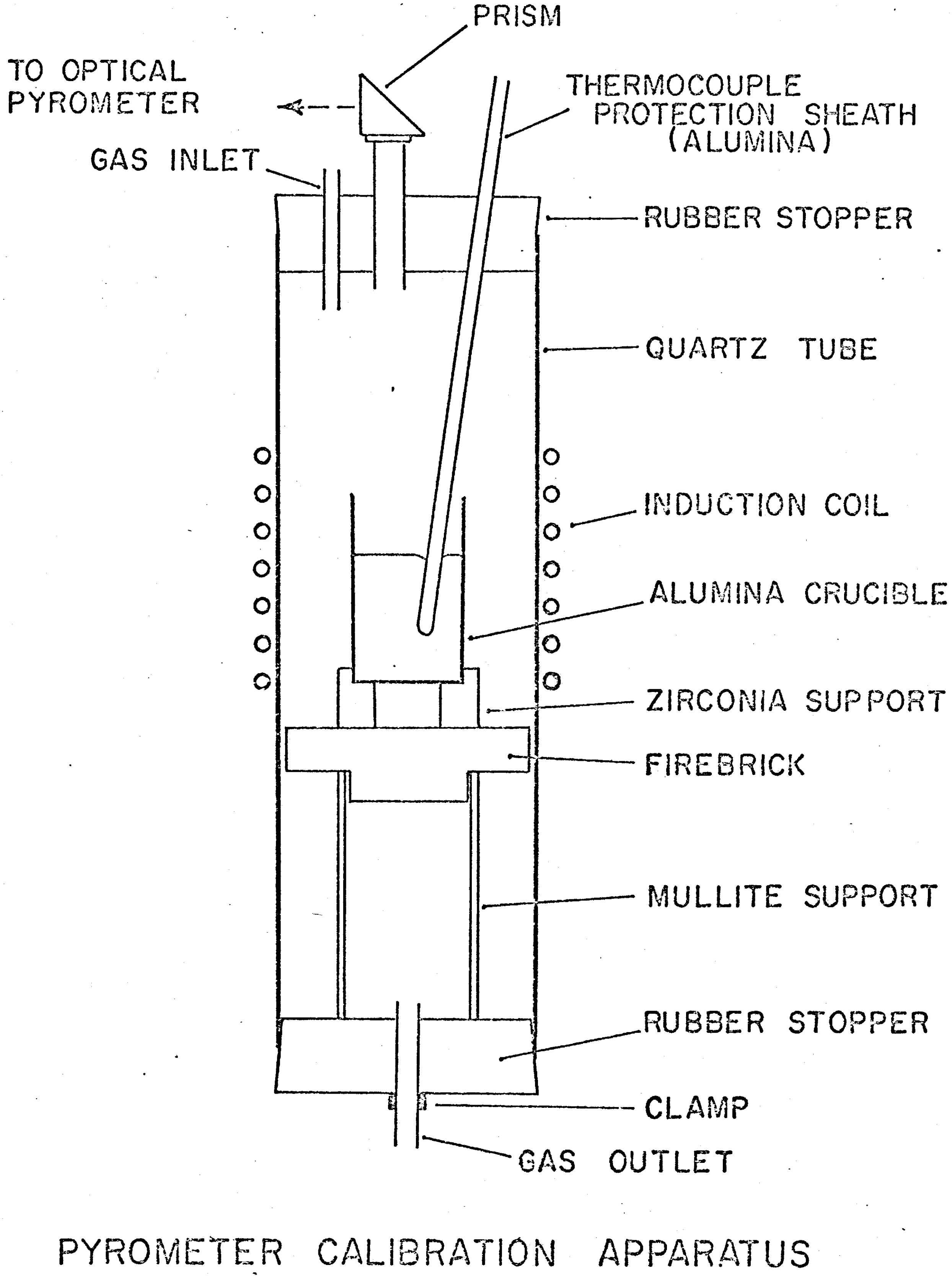

Figure 4a. Pyrometer calibration apparatus.

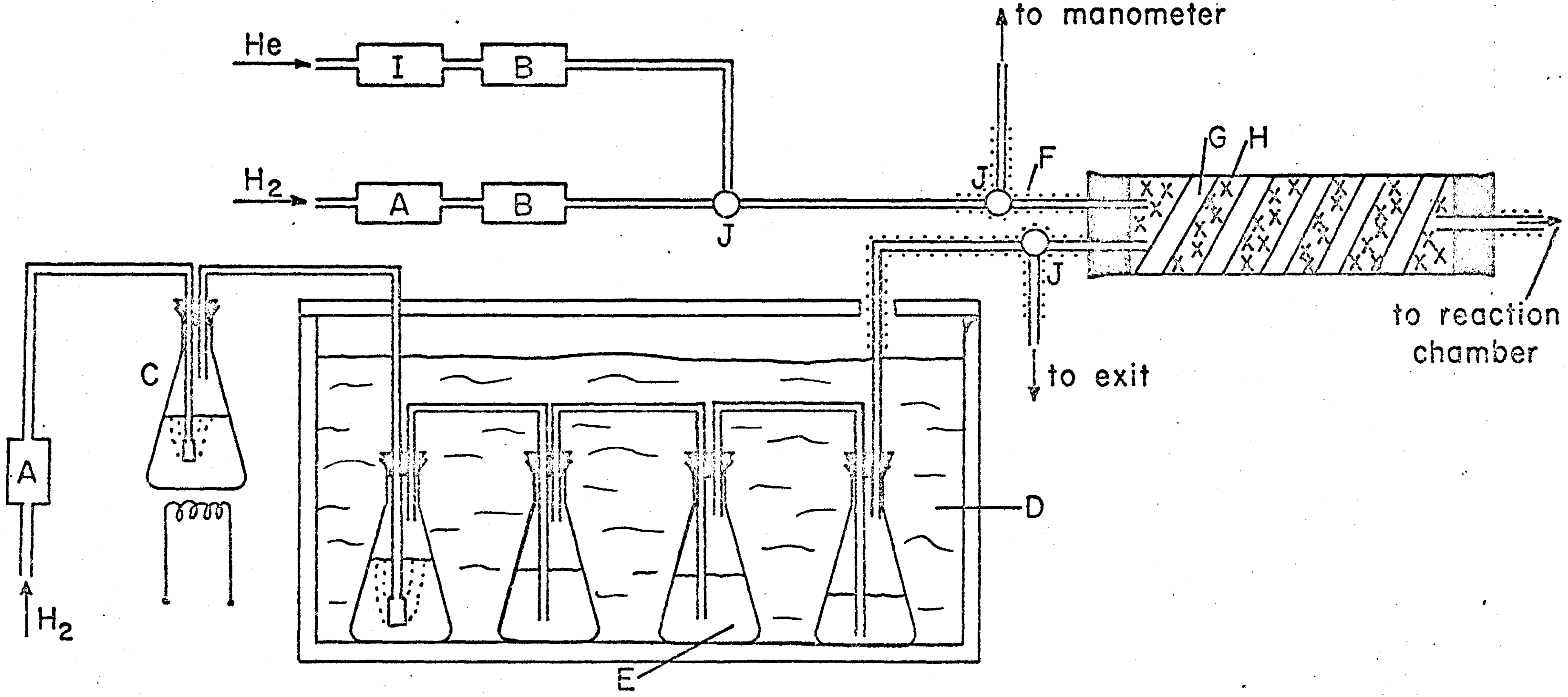

A	Palladium catalyst
B	Magnesium perchlorate
C	Presaturator
D	Water bath
E	Distilled water
F	Nichrome wire
G	Heating tape
H	Mixer filled with beryl saddles
I	Ascarite
J	Stopcocks

Figure 6. H_2-H_2O gas train (high and medium water vapor content).

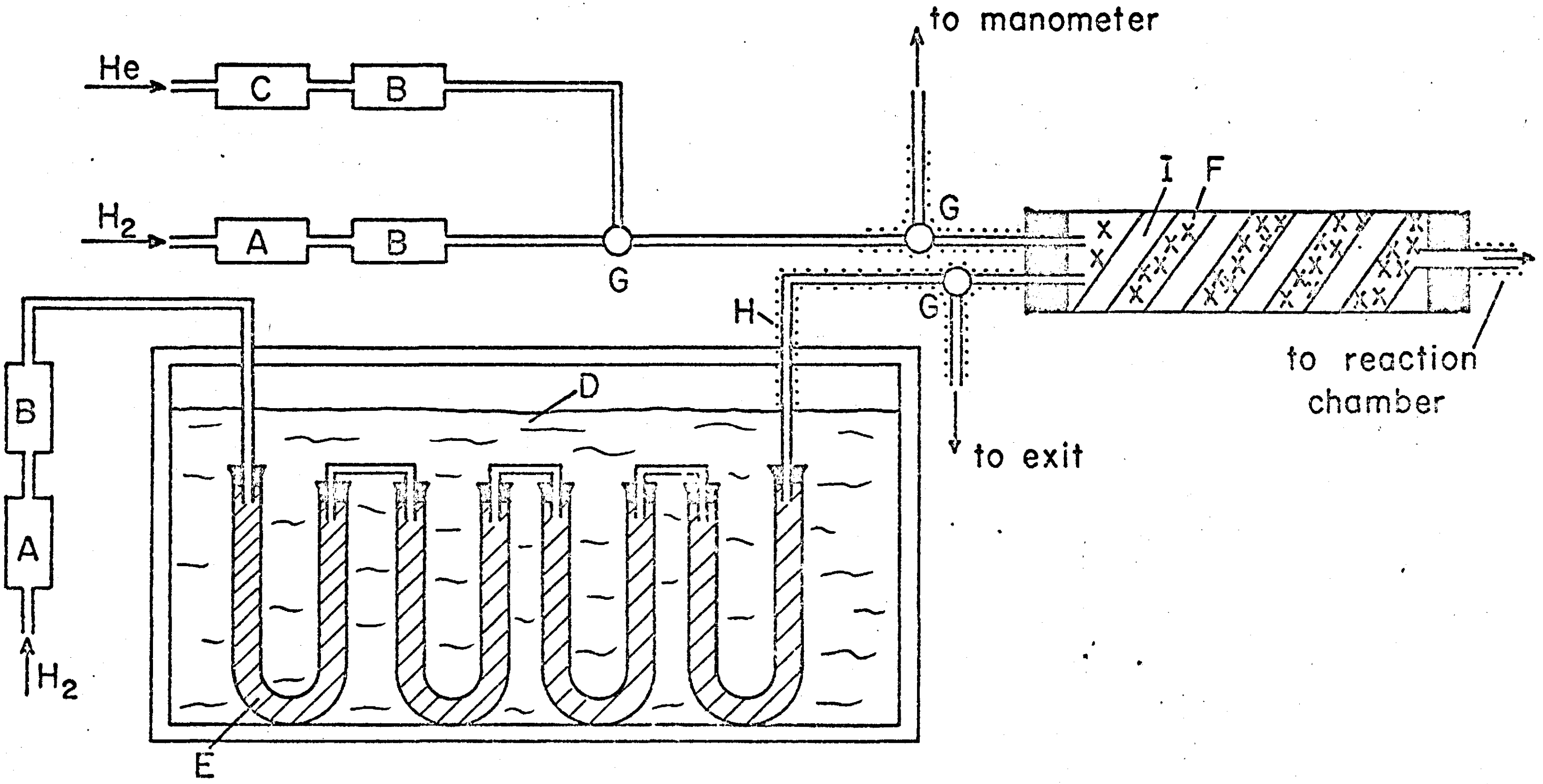

A	Palladium catalyst
B	Magnesium perchlorate
C	Ascarite
D	Water bath
E	Oxalic acid mixture
F	Mixer
G	Stop cocks
H	Nichrome wire
I	Heating tape

Figure 7. H_2-H_2O gas train (low water vapor content).

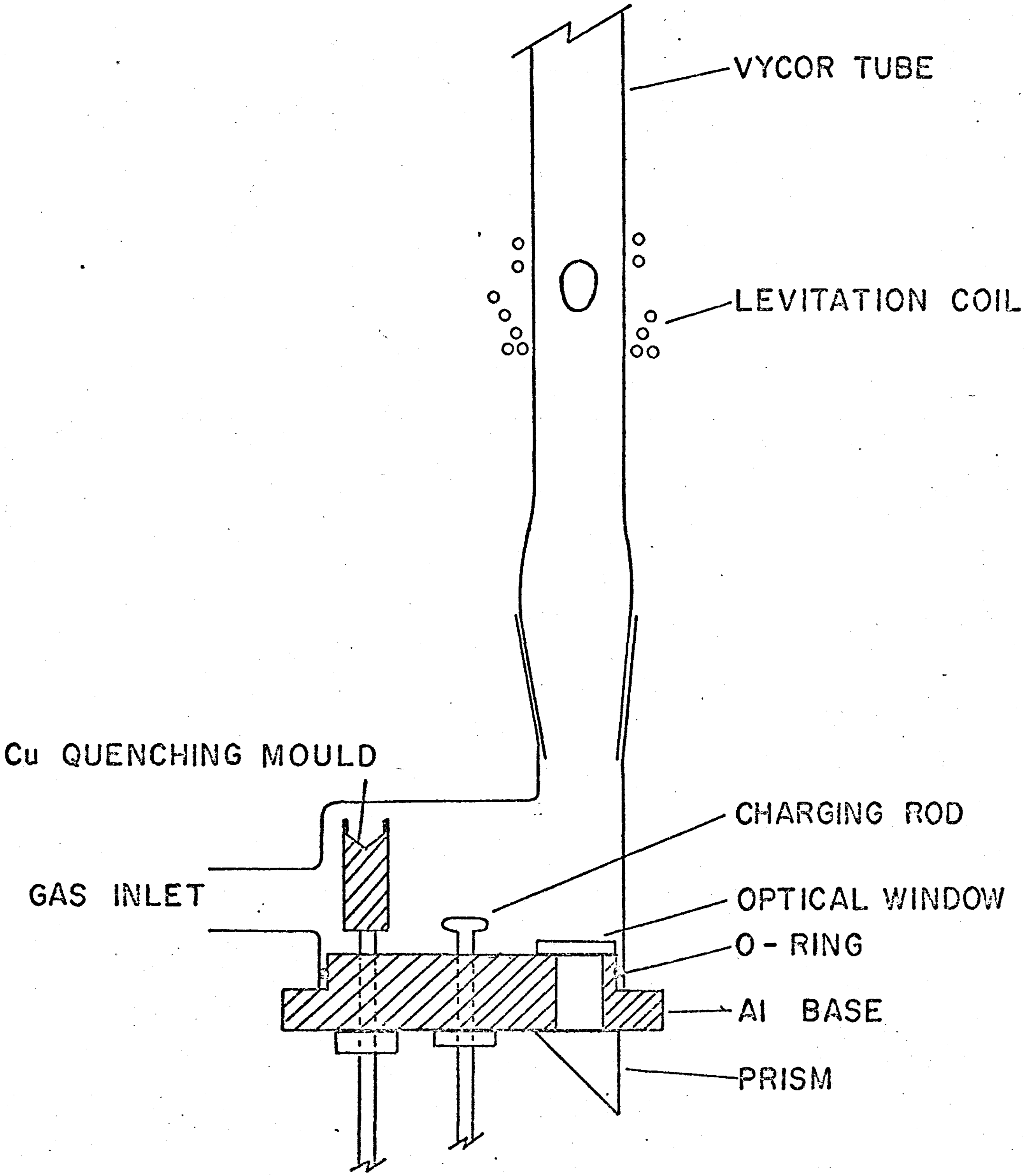

Figure 8. Reaction chamber with copper mold quenching.

Figure 9. Copper mold and quenched specimen.

Figure 10. Split mold. Lateral view of outside piece and inside piece - bottom view of quenched specimen.

Figure 11. Split mold. Top view of inside piece.

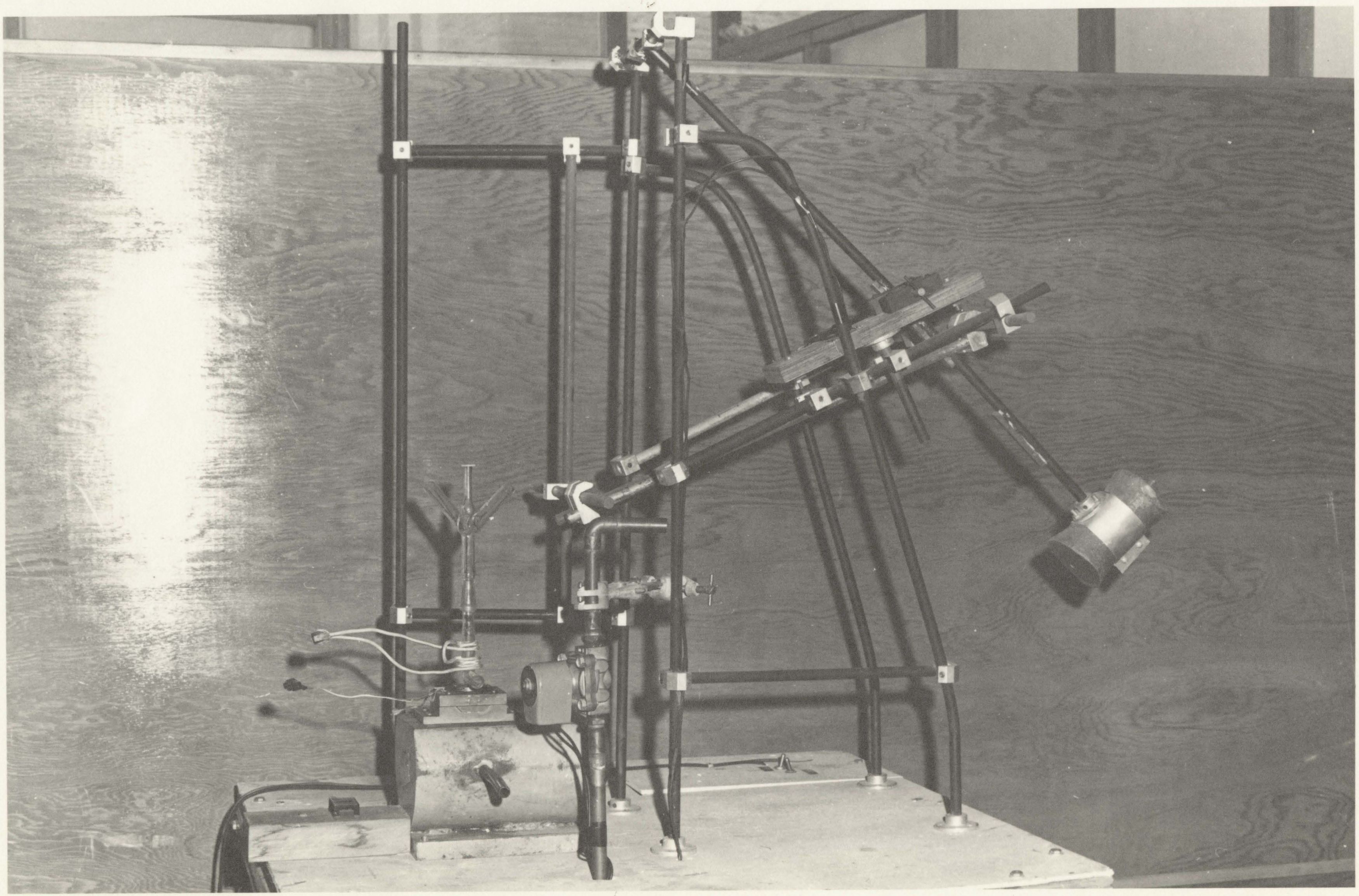

Figure 12. Piston and envil quenching mechanism.

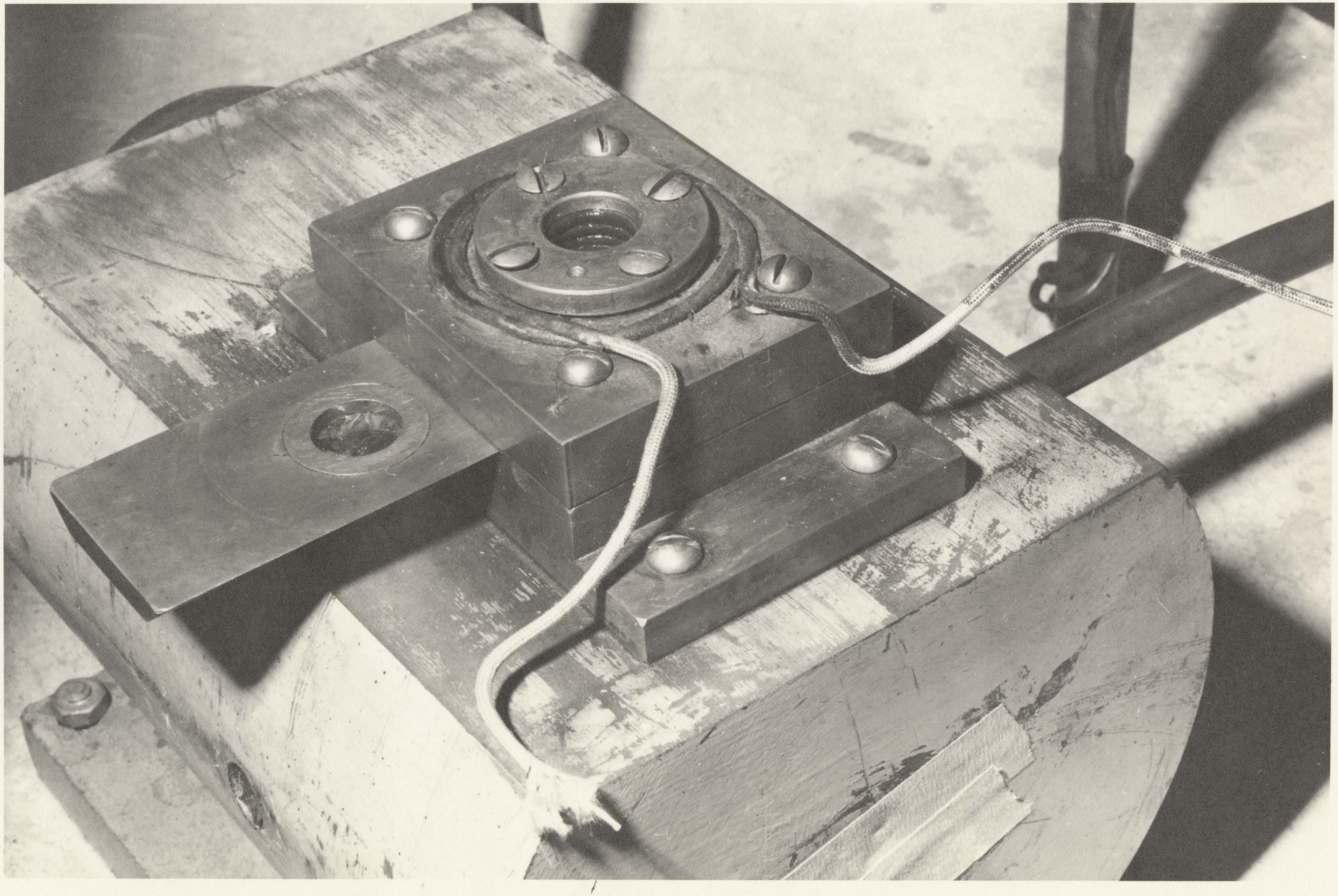

Figure 13. Close-up of the sliding valve.

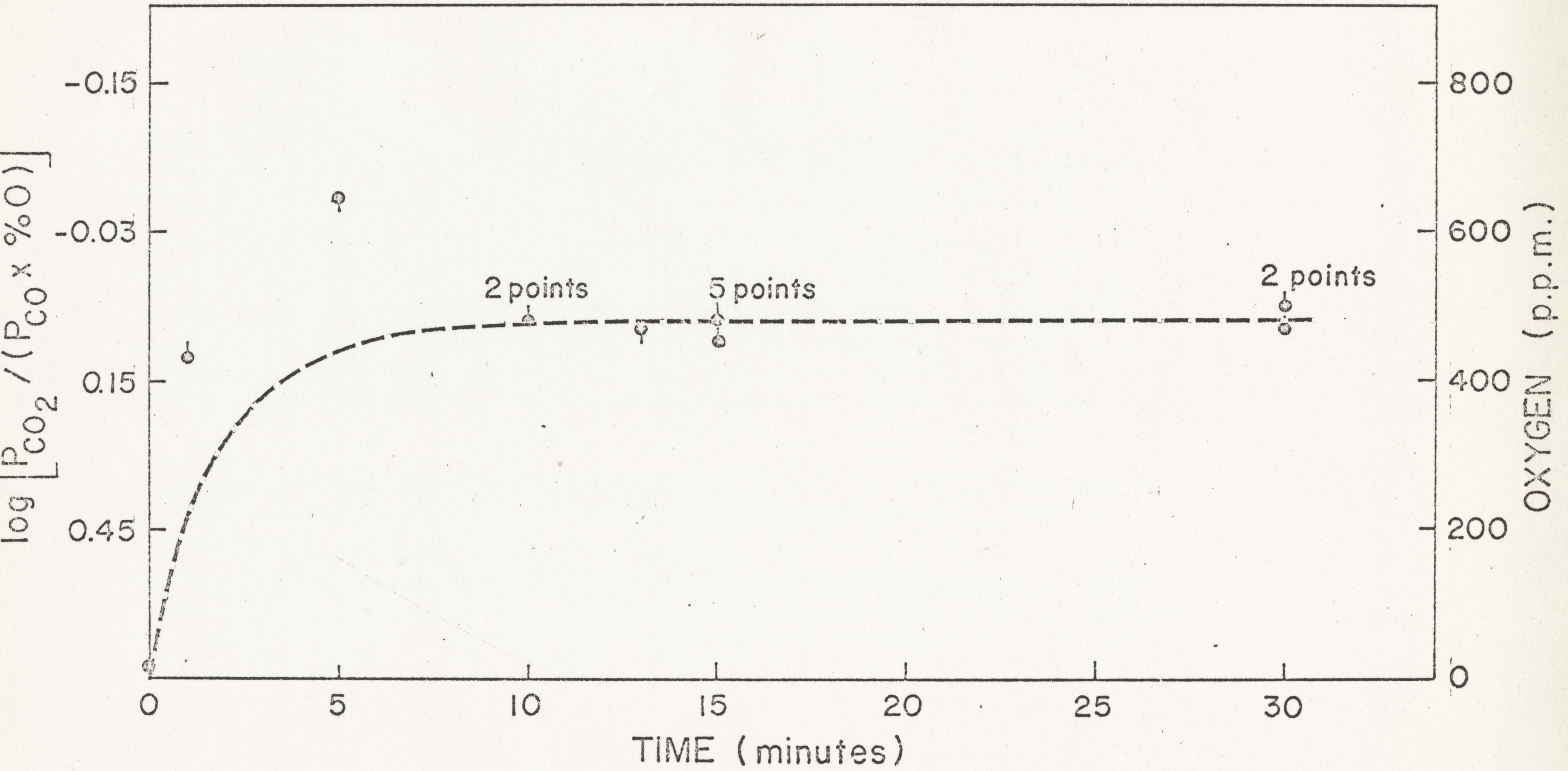

Figure 14. Attainment of equilibrium at 1550°C.

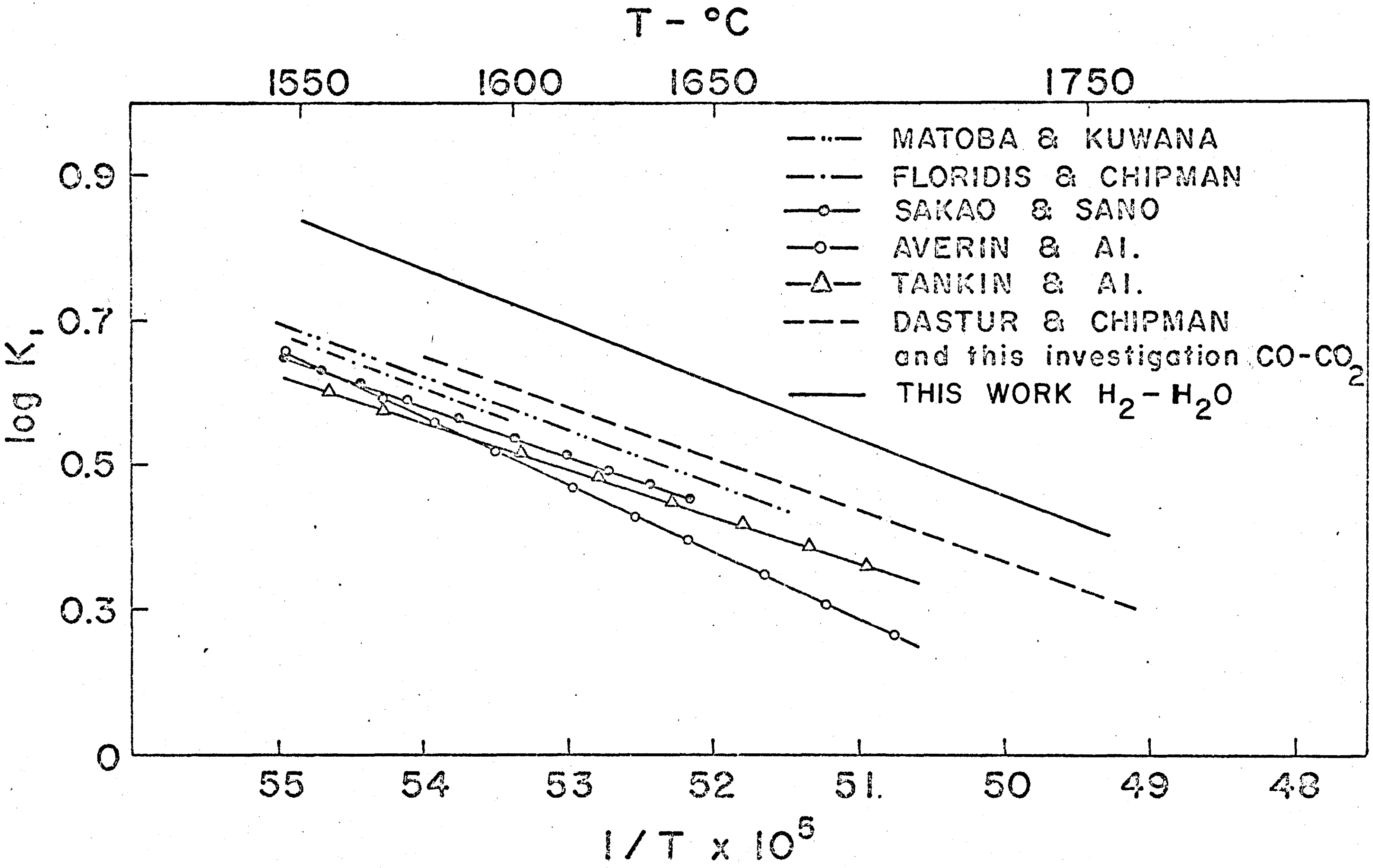

Figure 15. Variation of log K_1 with temperature.

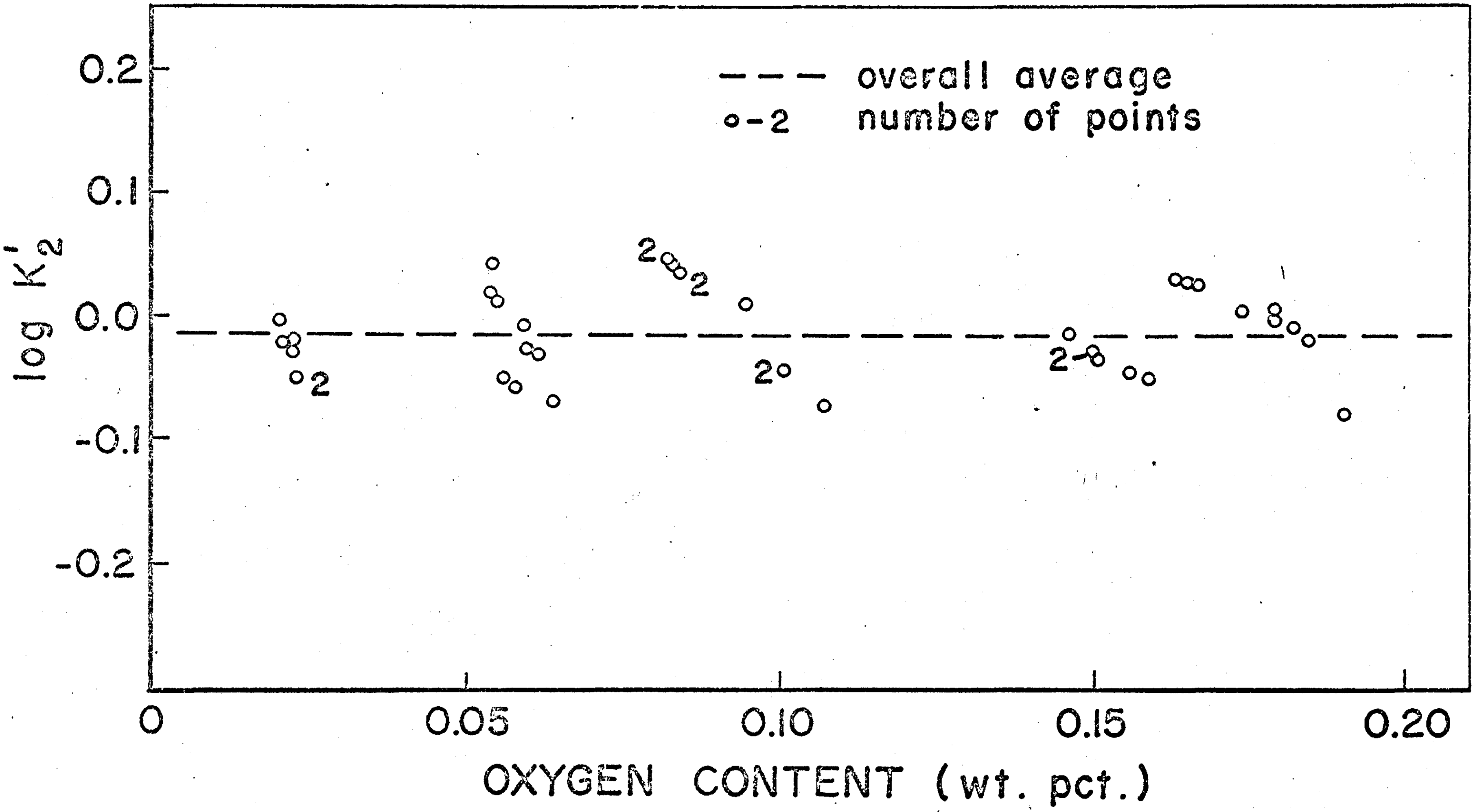

Figure 16. Effect of oxygen content upon log K'_2.

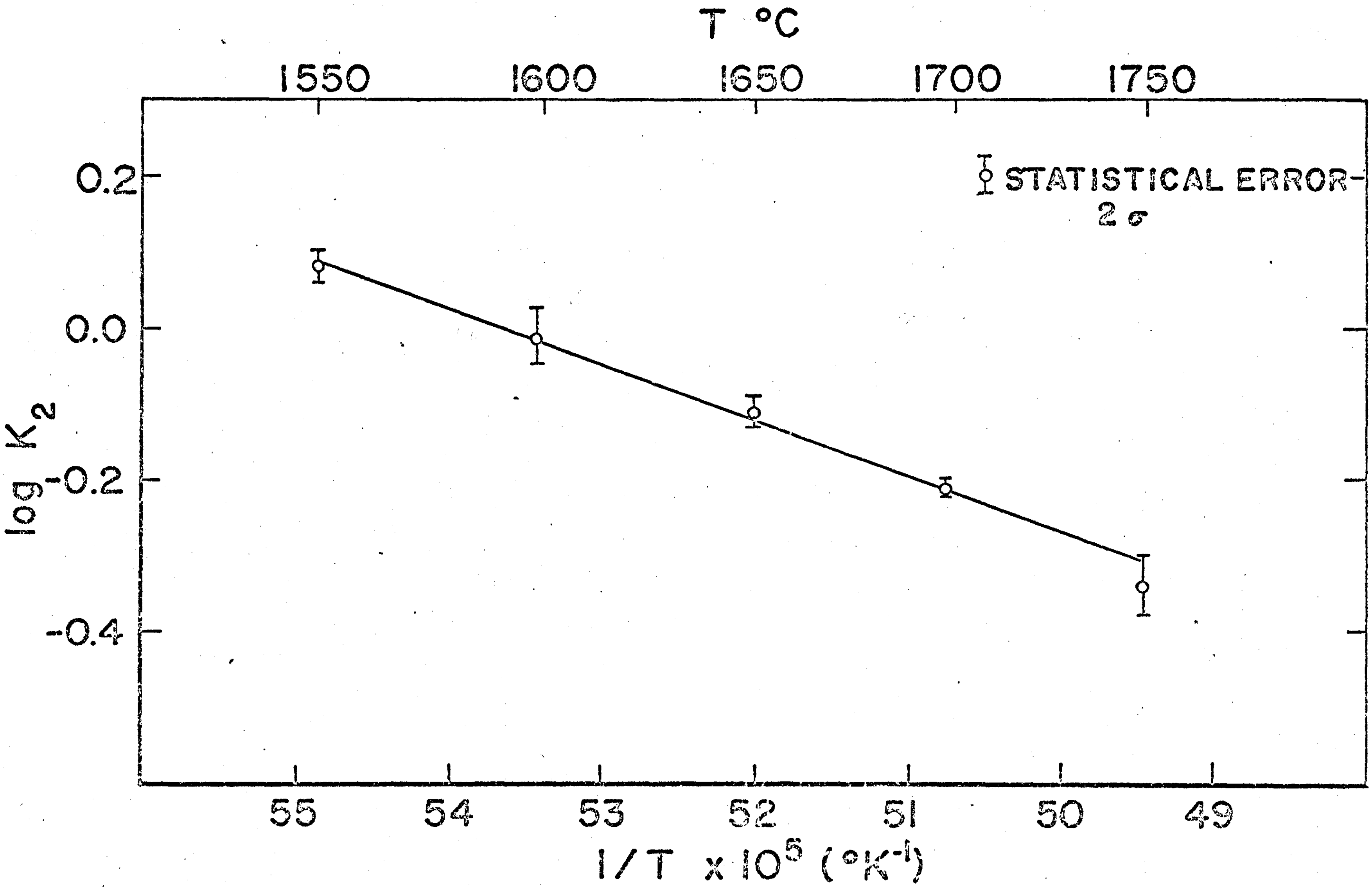

Figure 17. log K_2 versus temperature.

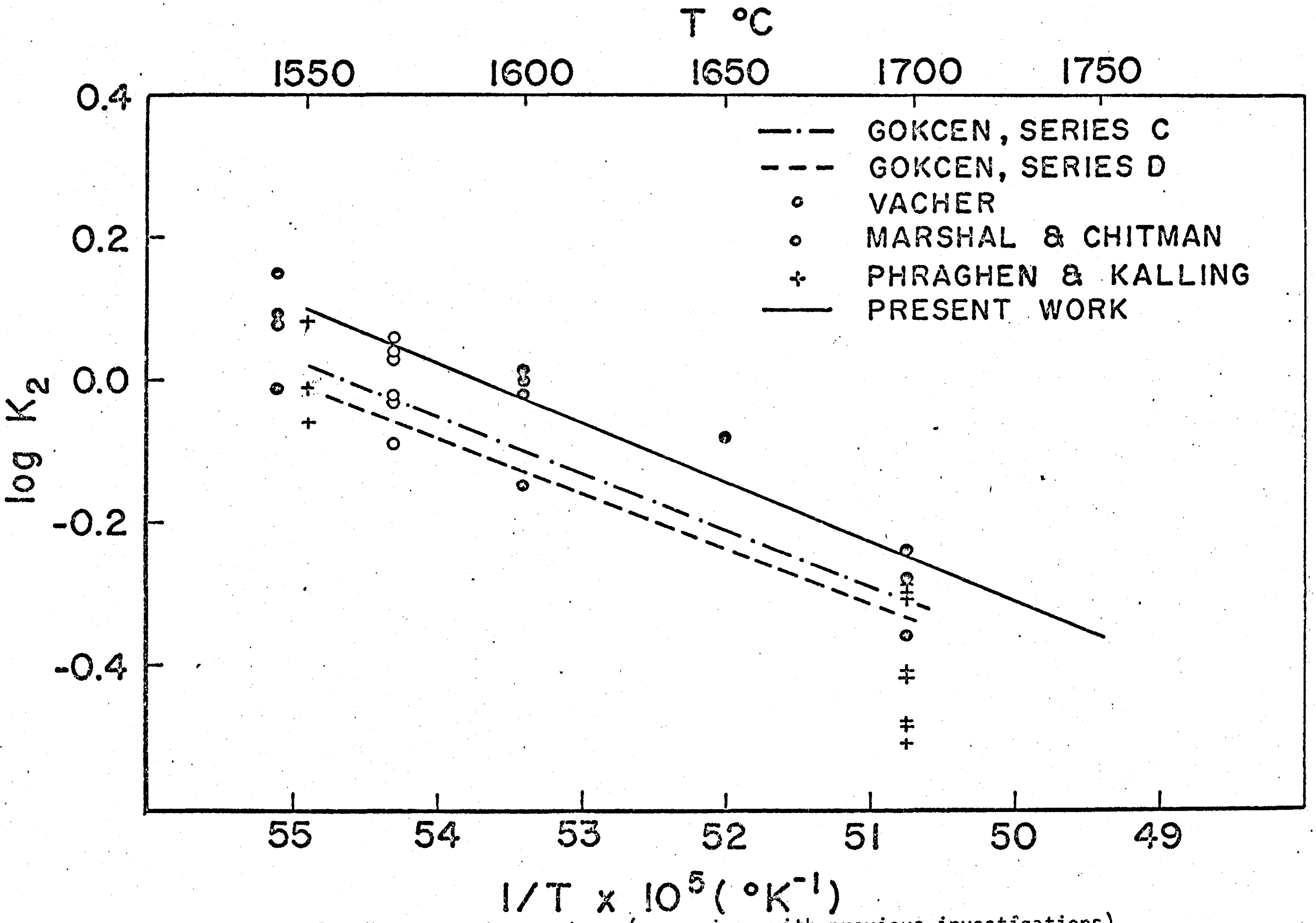

Figure 18. log K_2 versus temperature (comparison with previous investigations).

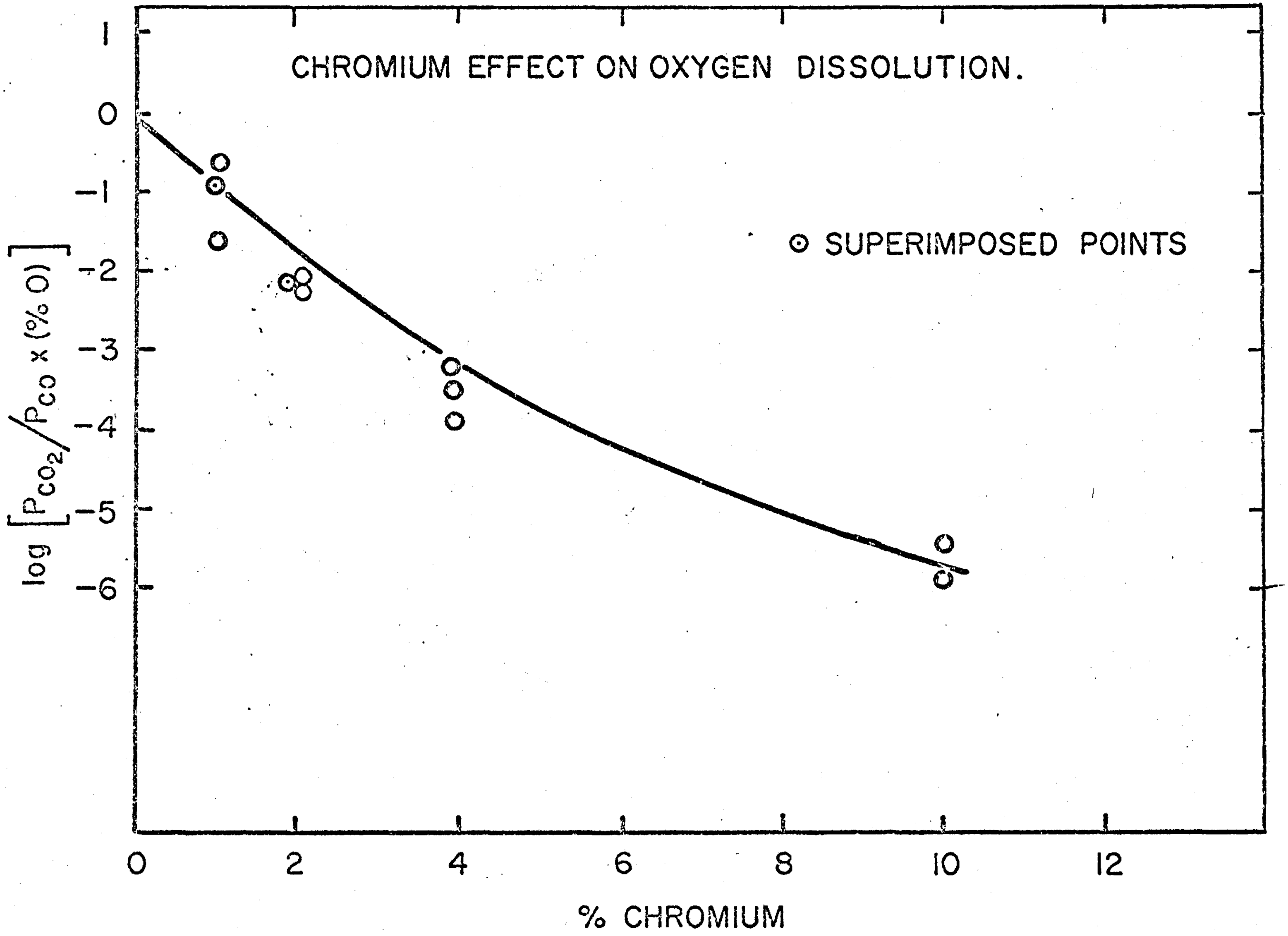

Figure 19. Effect of chromium on log K'_2 - temperature 1600°C.

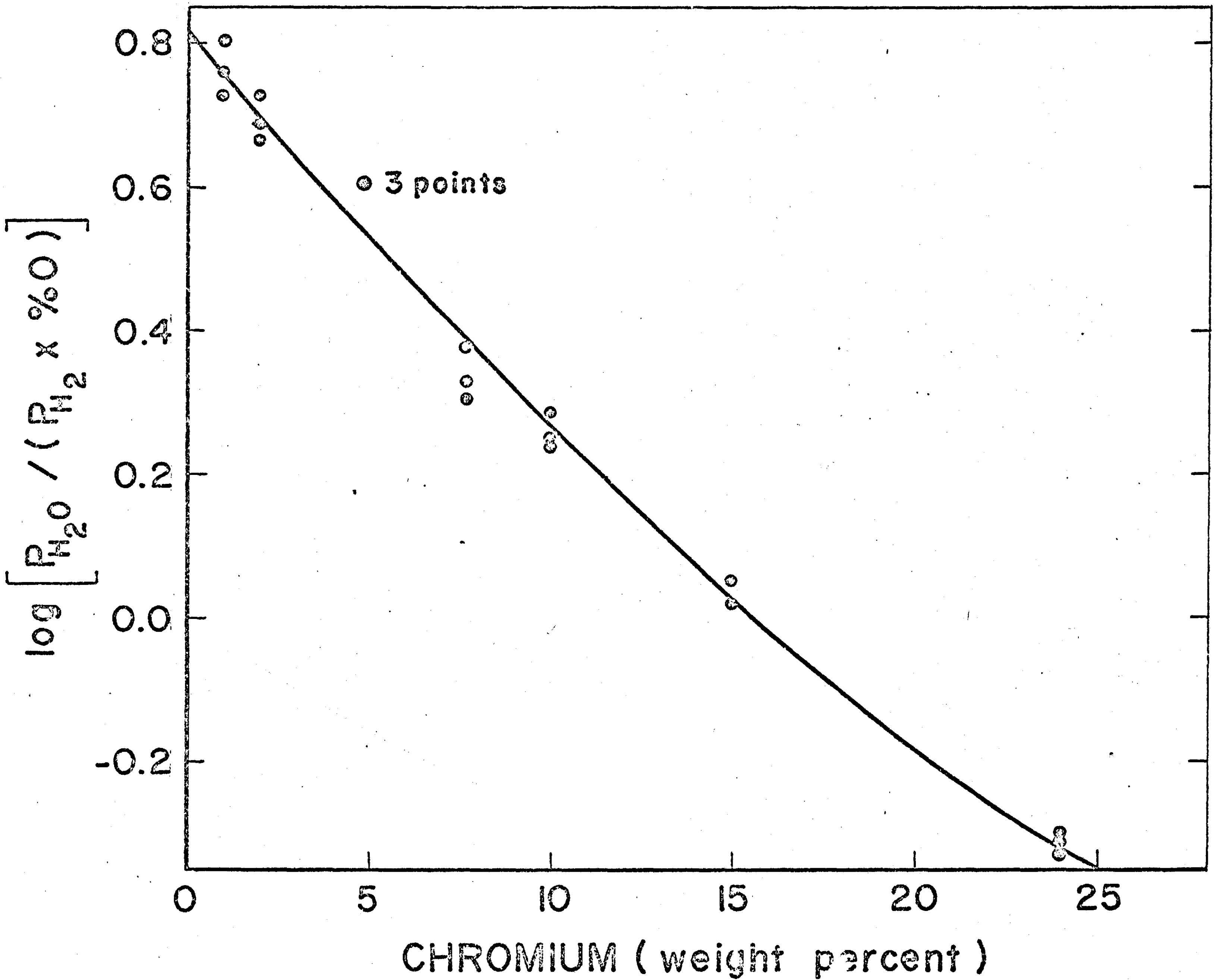

Figure 20. Effect of Cr on log K'_1 - temperature 1550°C.

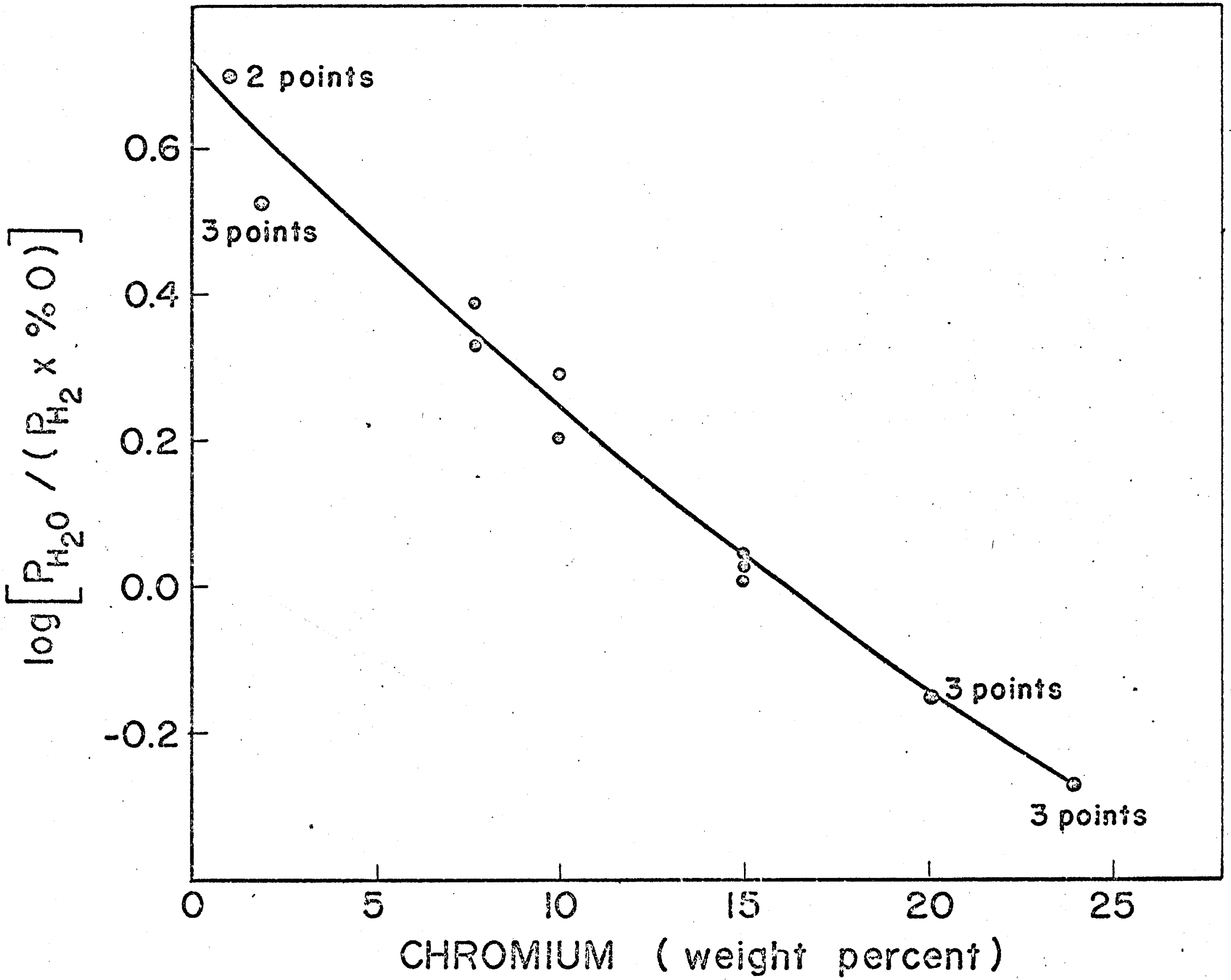

Figure 21. Effect of Cr on log K'_1 - temperature 1600°C.

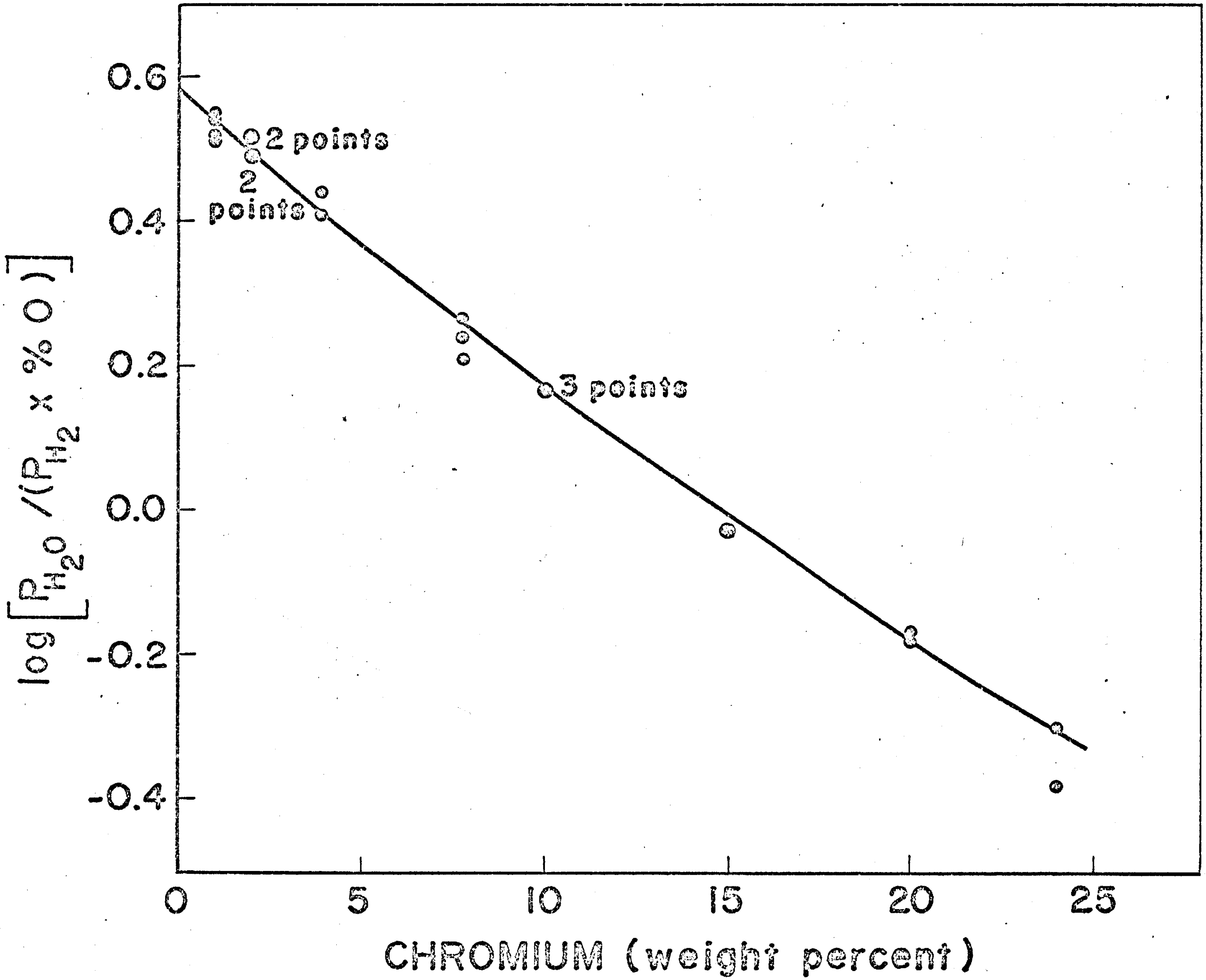

Figure 22. Effect of Cr on log K'_1 - temperature 1650°C.

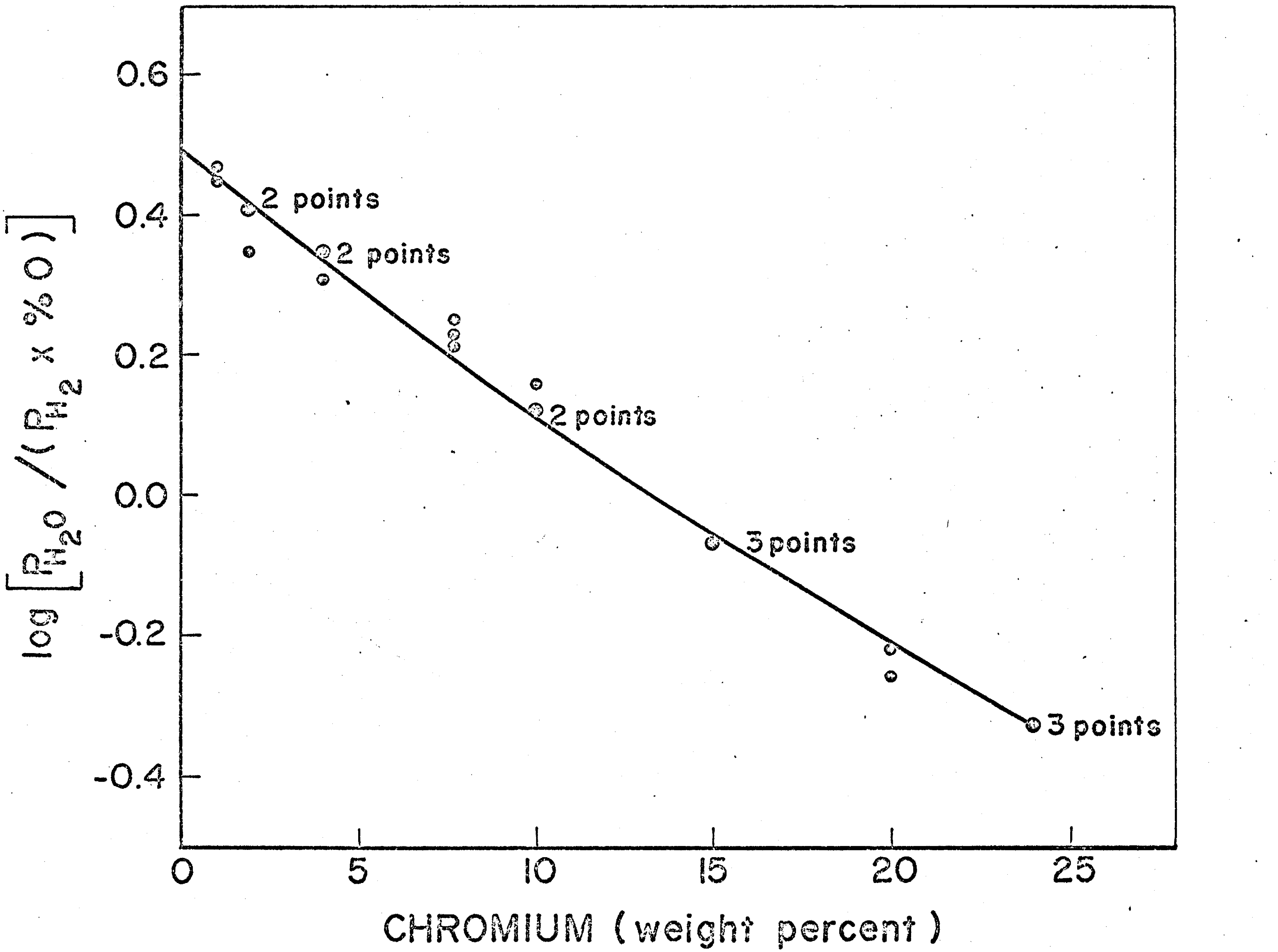

Figure 23. Effect of Cr on log K'_1 - temperature 1700°C.

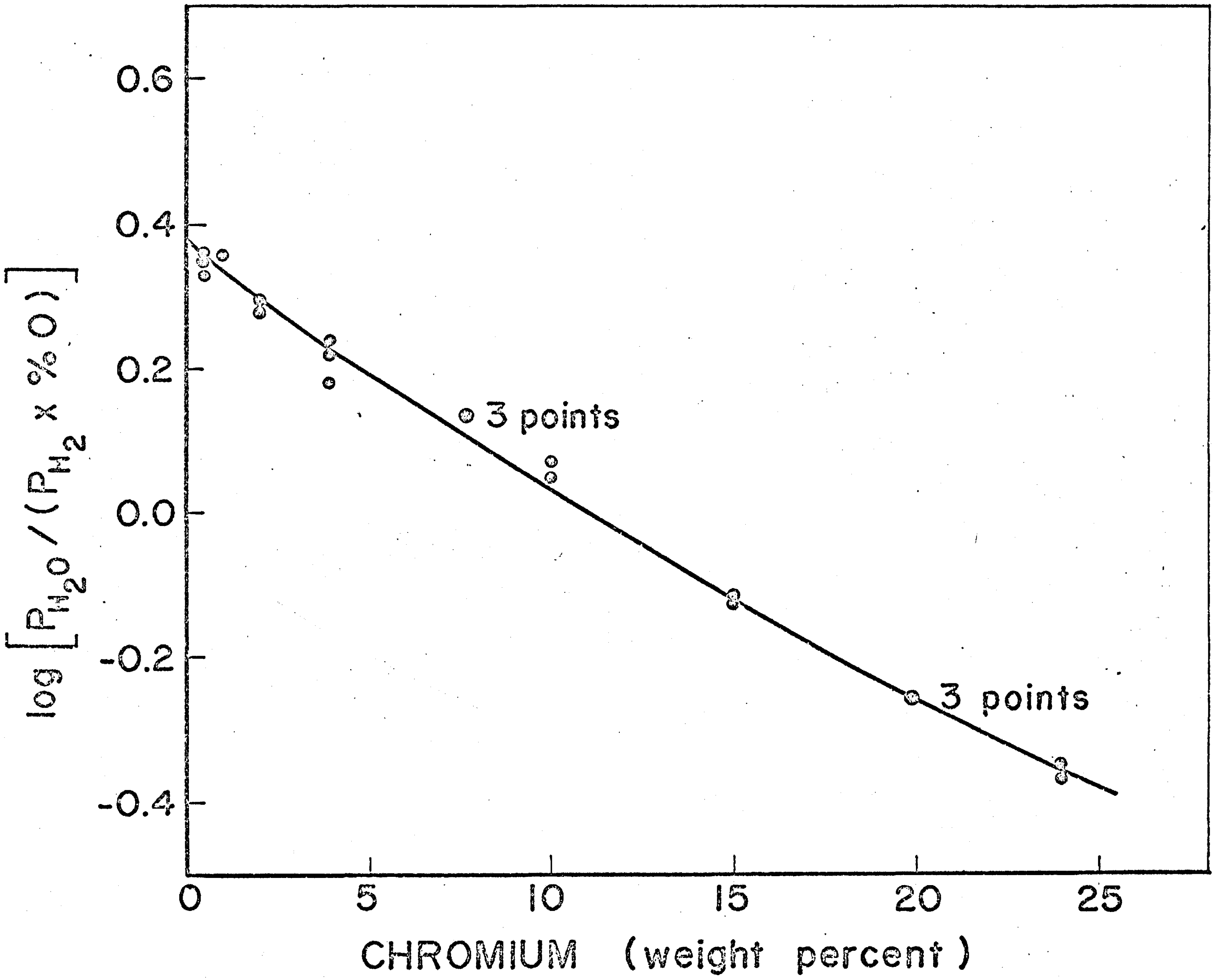

Figure 24. Effect of Cr on log K'_1 - temperature 1750°C.

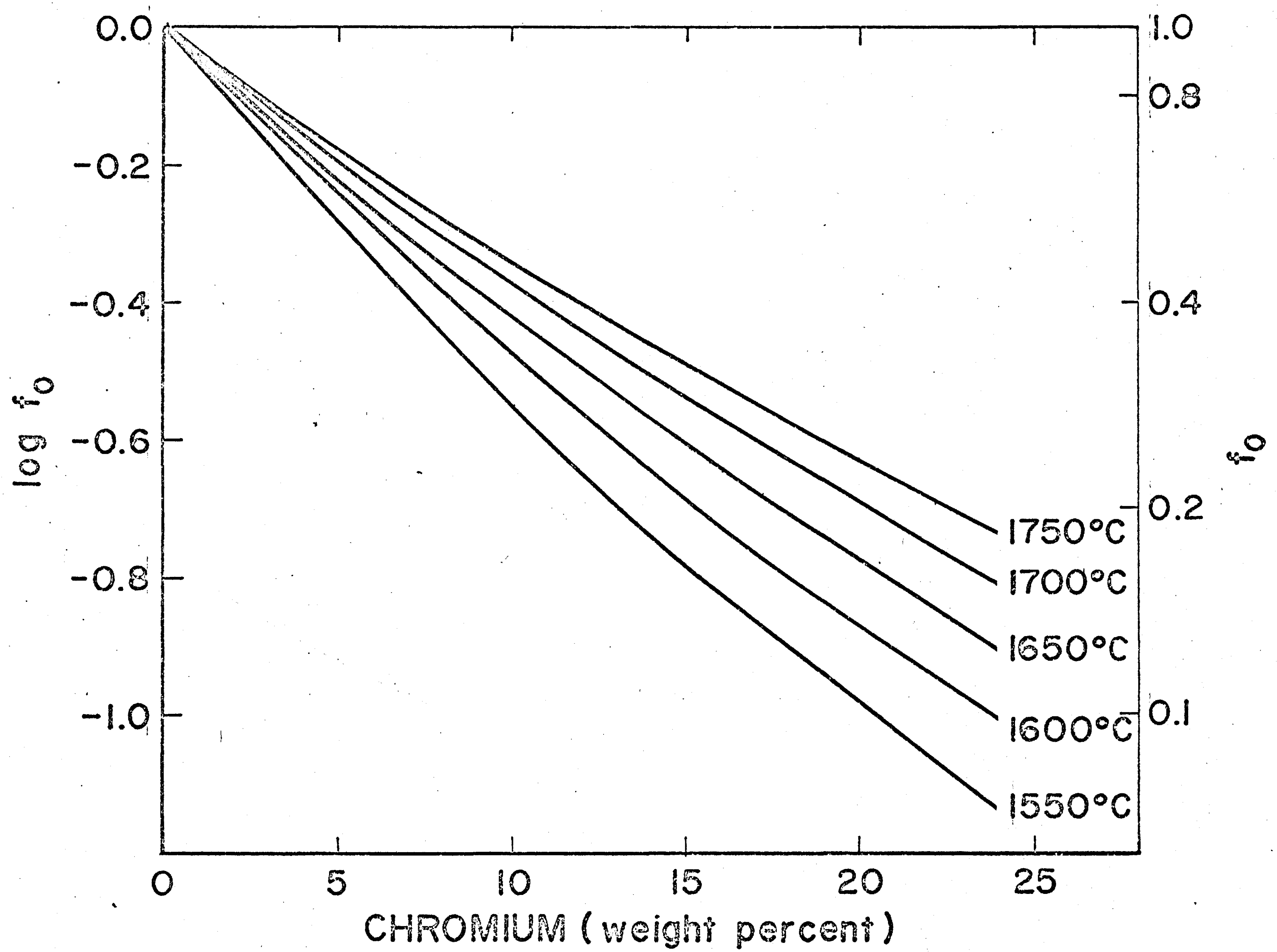

Figure 25. Activity coefficient of oxygen in Fe-Cr alloys.

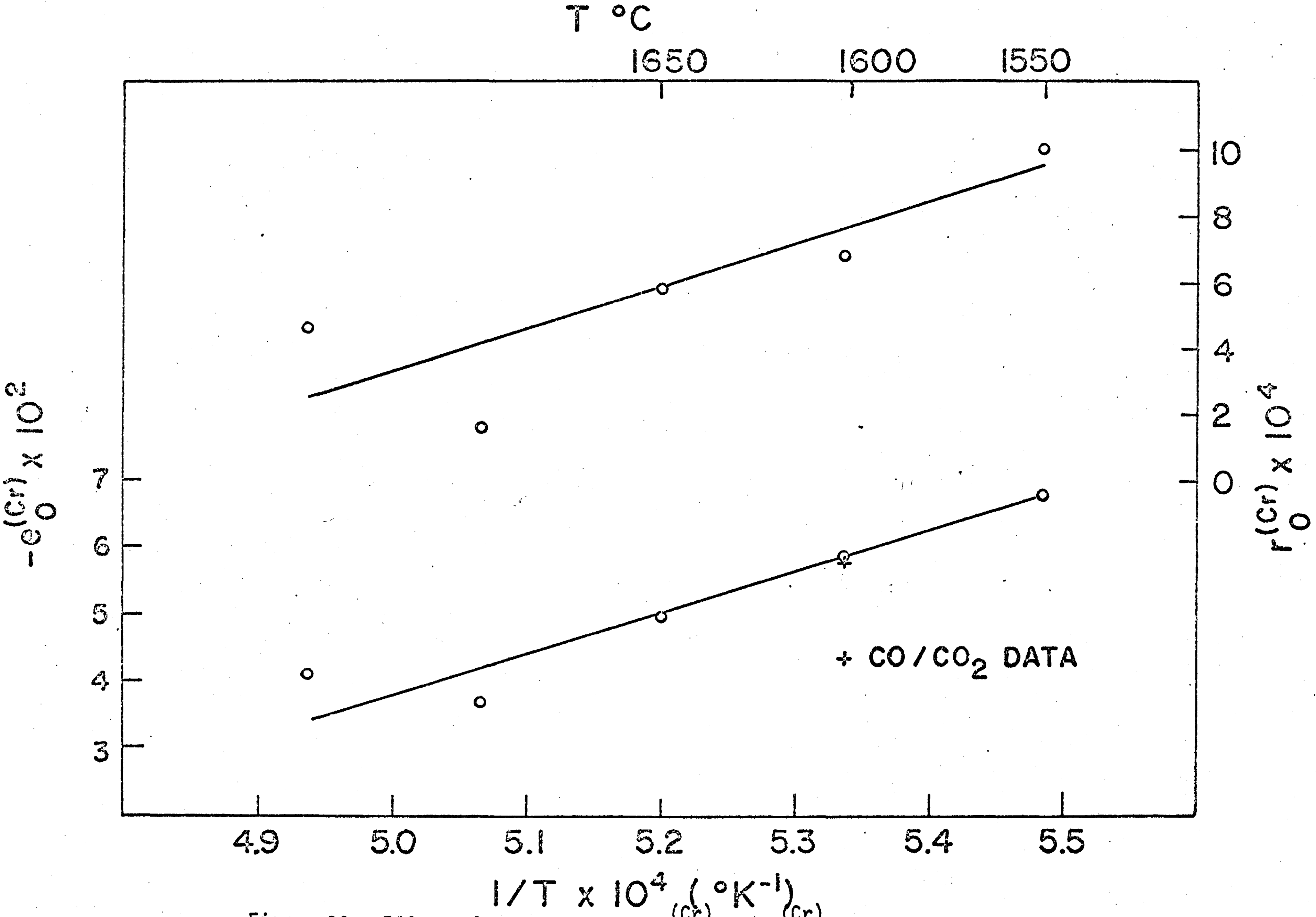

Figure 26. Effect of temperature on $e_0^{(Cr)}$ and $r_0^{(Cr)}$

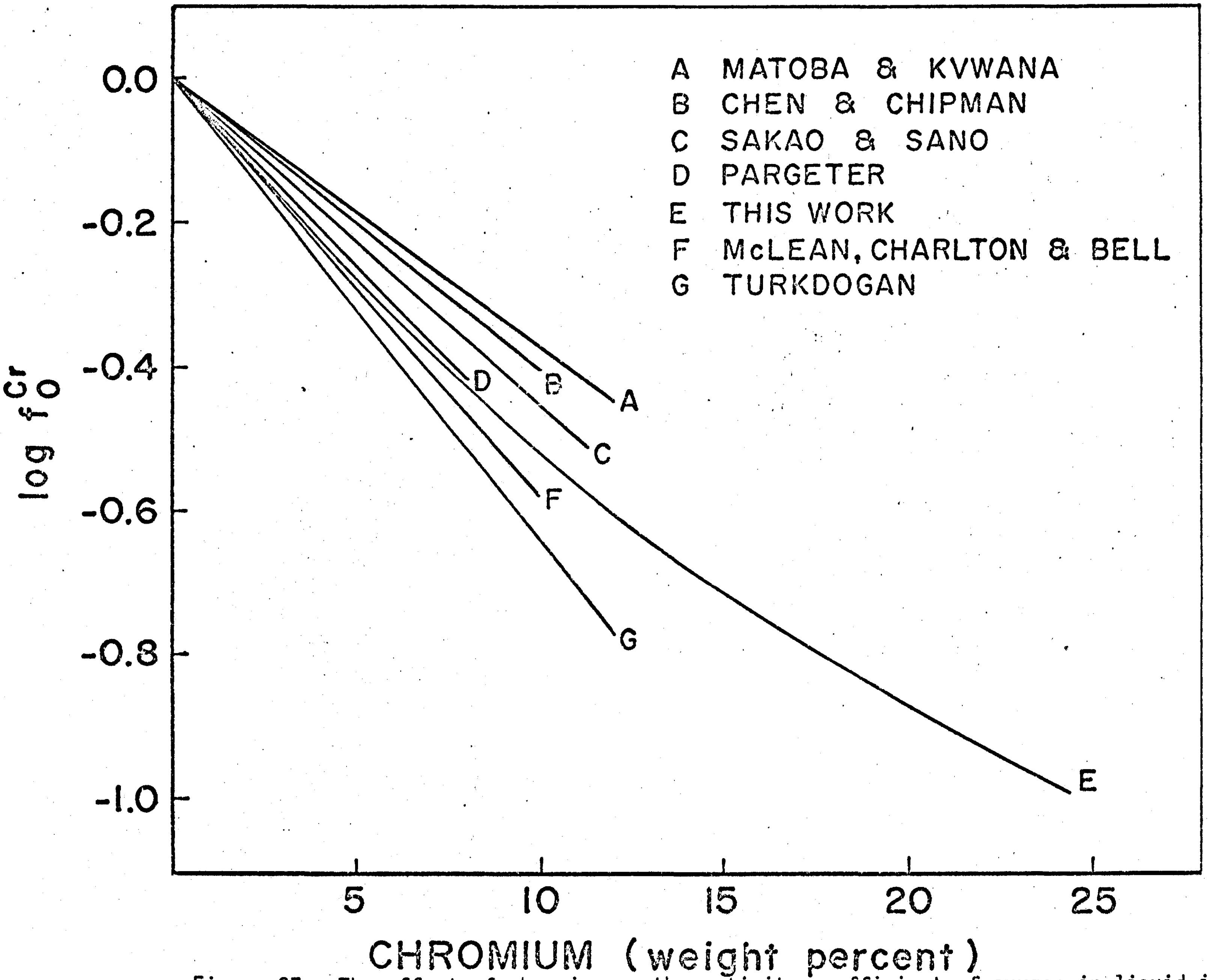

Figure 27. The effect of chromium on the activity coefficient of oxygen in liquid iron at 1600°.

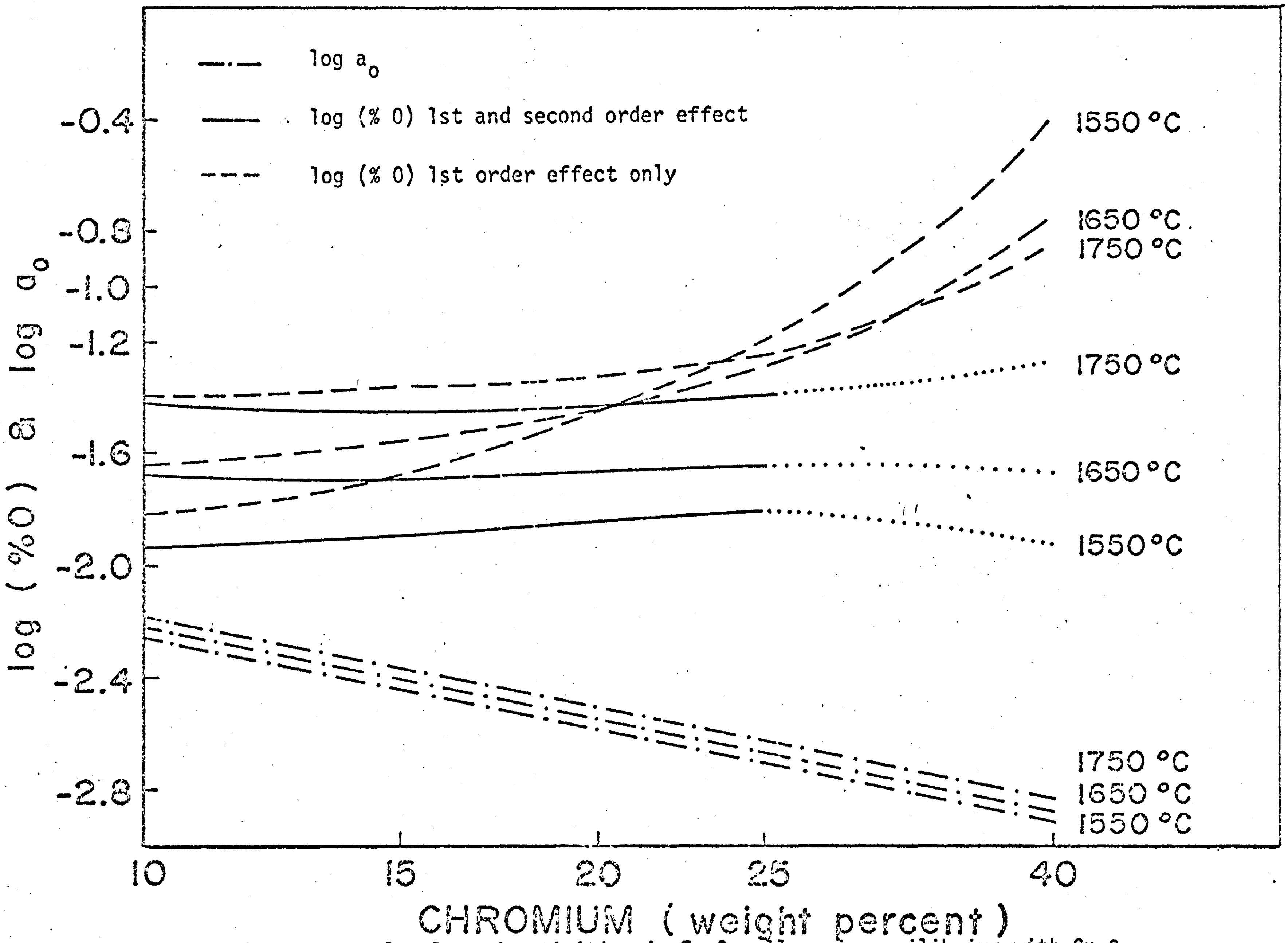

Figure 28. Oxygen levels and activities in Fe-Cr alloys in equilibrium with Cr_3O_4.

A	Magnesium Perchlorate
B	Palladium Catalyst
C	Ascarite
D	Optical Pyrometer
E	Levitation coil

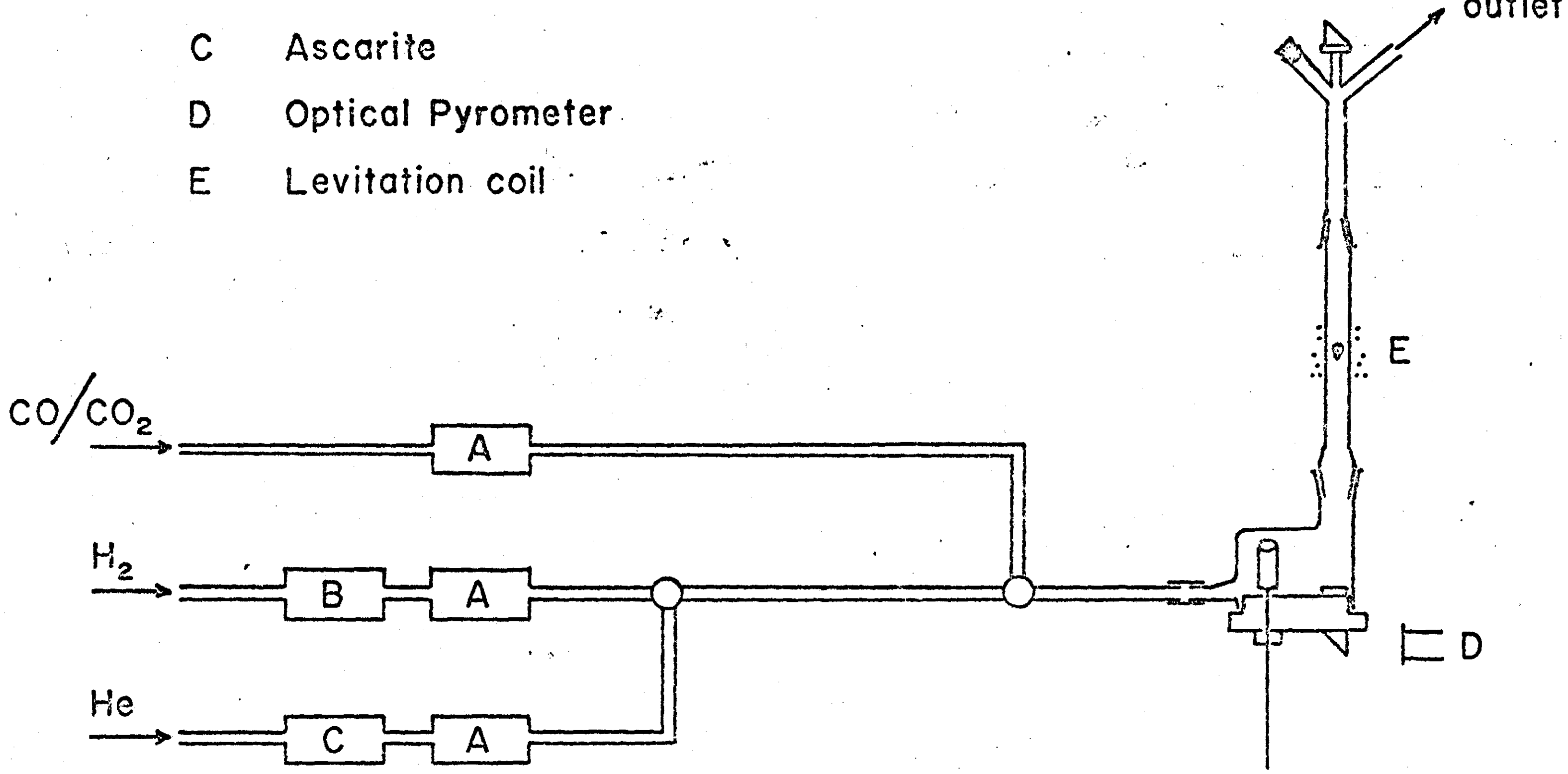

Figure 5. CO-CO$_2$ gas train.